Formulation development of a recombinant VAR2-antiCD3 protein for cancer immunotherapy

KLGM15: Master thesis in Pharmaceutical technology | 2021-04-22

Maja Warlin & Frida Hallberg, LTH, VAR2 Pharmaceuticals, CMC assist

Company supervisor (CMC Assist): Mette Hamborg
Laboratory supervisor (VAR2 pharmaceuticals): Ali Salanti
LTH supervisor: Jenny Schelin
LTH examiner: Marie Wahlgren

Executive summary

The use of immunotherapy for treating cancer has received a lot of attention in the recent years. The therapy is based on activating or deactivating the patient's own immune system to help fight the disease. One way of doing this, is using bispecific molecules that can target both cancer cells and T-cells simultaneously.

In 2003, a researcher found that the surface protein VAR2, expressed on malaria infected erythrocytes, could also specifically bind cancer cells. An idea came to mind to combine this protein with a scFv of the antibody aCD3, for immunotherapy targeting cancer. This rVAR2-aCD3 fusion protein was the start of the company VAR2 Pharmaceuticals. Today, the product has been developed and the company is hoping to start clinical trials in the near future.

The aim of this master thesis was to select the best candidate for a frozen-liquid rVAR2-aCD3 buffer formulation to be used in clinical phase I studies. The method included 10 analytical techniques measuring different properties correlated to stability. SE-HPLC and SDS-PAGE were used to examine aggregation, degradation and contamination. Size distribution was studied using DLS and SEC-MALS. Furthermore, SEC-MALS and MS was used to determine the molar mass. Protein concentration was measured in NanoDrop and unfolding correlated to temperature was examined in NanoDSF. ELISA and FACS were used to investigate binding. Lastly, a fractionation of monomer and dimer was performed using NGC.

At the start of the study, the stability effect on the protein of six different buffers with pH ranging from 3-8, stored in -80°C versus 4°C respectively, were examined. A final formulation was systematically down selected through three consecutive sub studies, investigating pH dependence, tonicity and physical stress.

In the initial study it was found that low pH (3.3-4.5) seemed to destabilize the protein. Using NanoDSF, it was also found that the unfolding process related to increased temperature seemed to be pH dependent. Buffers with a pH <7 tended to unfold in two steps whereas buffers with a pH >7 unfolded in one single step. From the tonicity study, it was found that both sucrose and NaCl could work as tonicity providers to the fusion protein. However, the combination of histidine buffer and sucrose seemed to have negative effects on the desalting process. Also, it was seen that the samples stored in -80°C were more stable than the samples stored in 4°C. The formulation with PBS, tris-HCl with sucrose and histidine buffer with NaCl showed to be stable all through the 5 weeks of which the tonicity sub-study was performed.

In the final stress study, it was found that the protein was stable towards freezing and thawing up to 6 times. Furthermore, storage at room temperature and rotation caused aggregation and degradation which was found in SDS-PAGE and SE-HPLC measurements. The histidine buffer with NaCl seemed to be most stress resistant with the least aggregation and degradation products forming, keeping the highest monomer content over time and showing the highest binding towards the desired ligand decorin. Hence, histidine buffer with 150mM NaCl was chosen as the best candidate for a frozen-liquid rVAR2-aCD3 buffer formulation to be used in clinical phase I studies.

Table of contents

1. Abbreviations

APC = antigen presenting cells
Asn = asparagine
Asp = aspartic acid
BiTE = bispecific T-cell engager
BSA = bovine serum albumin
CDR = complementarity-determining region
CS = chondroitin sulfate
CSA = chondroitin sulfate A
DBL = duffy binding like
DLS = dynamic light scattering
DTT = dithiothreitol
ELISA = enzyme-linked immunosorbent assay
FACS = fluorescence-activated single cell sorting
Fc region = fragment crystallizable region
FT= freeze-thaw
Gln = glutamine
Gly = glycine
Ig = immunoglobulin
IgG = immunoglobulin G
kDa = kilo Daltons
mAb = monoclonal antibody
MES = (2-(N-morpholino) ethanesulfonic acid
Met = methionine
MHC = major histocompatibility complex
MS = mass spectrometry
NanoDSF = nano differential scanning fluorimetry
NK cell = natural killer cell
NMR = nuclear magnetic resonance
ofCS = oncofetal chondroitin sulfate
PBMC = peripheral blood mononuclear cells
PBS = phosphate buffered saline
Pro = proline
ScFv = single chain variable fragment
SDS-PAGE = sodium dodecyl sulfate polyacrylamide gel electrophoresis
SEC MALS = size exclusion chromatography multi angle light scattering
SE-HPLC = size exclusion high pressure liquid chromatography
Ser = serine
rVAR2-aCD3 = recombinant VAR2-aCD3
TCR = T-cell receptor
TILs = tumor-infiltrating lymphocytes
TP = time point
Tris-HCl = tris(hydroxymethyl) aminomethane

2. Introduction

In today's society, cancer is one of the main causes of death across the world (World health organization, 2020). A treatment for cancer that has received a lot of attention in recent years is immunotherapy, which was awarded the Nobel Prize Physiology or Medicine in 2018 (The Nobel Prize, 2018). VAR2 Pharmaceuticals is a small company located in Copenhagen, Denmark, developing a new type of cancer immunotherapy treatment using the malaria protein recombinant (r) VAR2 to target cancer cells. The protein is fused together with the antibody aCD3 that binds T-cells, making up the rVAR2-aCD3 protein which is the company's pharmaceutical product.

The scope of this project was to find the optimal formulation and storage environment of rVAR2-aCD3. In order to start phase I clinical studies, stability studies on a set of suggested formulations of rVAR2-aCD3 needed to be performed. VAR2 pharmaceuticals decided to do this in collaboration with the biotech consultancy firm CMC Assist. Through contacting CMC Assist, the idea behind this Master thesis came to form, including 20 weeks of full-time work for VAR2 pharmaceuticals with the aim of finding the best suited formulation for rVAR2-aCD3.

3. Aim

The aim of the Master thesis was to select the best candidate for a frozen-liquid rVAR2-aCD3 formulation to support clinical phase I studies. This was done by trying to find the optimal environmental conditions for rVAR2-aCD3 using a range of different analytical techniques to understand the physical characteristics of the protein. The project was divided into three sub studies, including an initial study, a tonicity study and a stress study. In addition, an *in silico* protein observation was performed for better understanding of the chemical structure of the recombinant protein.

Objectives

- Study how different formulation parameters such as pH, buffer solution and additives affect the stability of the rVAR2-aCD3.
- Evaluate protein stability using different analytical techniques including NanoDrop, SDS-PAGE, ELISA, SE-HPLC, FACS, NanoDSF, SEC-MALS, NanoDLS, NGC and MS.
- Examine how the stability of the rVAR2-aCD3 protein is impacted under different types of stress (storage temperature, shear stress and freeze-thaw stress).

4. Theory

In the following sections, the theory behind the project is presented.

4.1 Proteins

Proteins stand out compared to other types of compounds used in the pharmaceutical industry in terms of having high molecular weight, large size, and compositional variety. Furthermore, they are special due to their amphipathic characteristics and possibility of unfolding and denaturing. Another important feature of

proteins is their high specificity and activity even in low concentrations. As there are many different environmental factors that can affect the activity and function of the proteins it is important to optimize their conditions to work in the most favorable way. (Wang, W., 1999)

4.1.1 Chemical and physical stability

Chemical and physical stability are linked in many ways even though there are clear differences separating them apart. Chemical stability involves the processes where covalent bonds are made or broken to create connections between new units. Physical stability on the other hand, involves processes where the physical state of the protein changes. These processes can for instance be denaturation, aggregation, precipitation and adsorption. (Manning, M. C., et al. 2010)

4.1.2 Protein folding and stability

Protein folding is usually divided into four different levels. The first level is the primary structure, which is the amino acid sequence. Upon that comes the secondary structure, referring to sub-structures the amino acids fold into such as alpha helices or beta sheets. The tertiary structure is the three-dimensional structure and lastly the quaternary structure, represents the full protein complex composed of different sub-structures. The levels are presented in figure 1 below. (Creative proteomics, 2021)

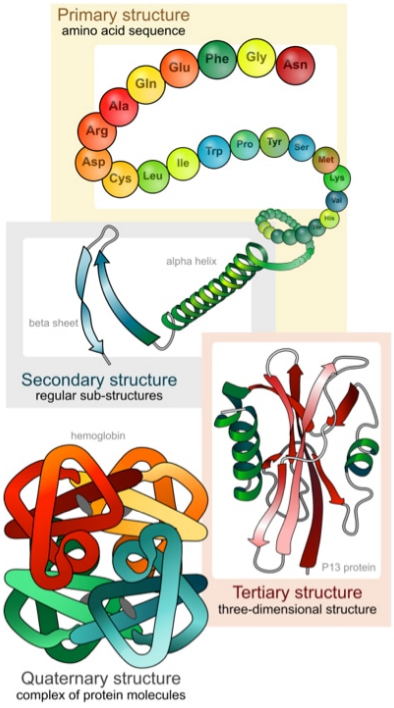

Figure 1. The four levels of protein folding: primary, secondary, tertiary and quaternary structure (Creative proteomics, 2021).

A protein can fold into many different three-dimensional conformations, however, only a limited amount of them are preferred by the protein itself. Commonly, the most preferred state is referred to as the native state of the protein - the conformation it has under native conditions. (Wang, W., 1999)

Protein folding is mainly governed by hydrophobic interactions and hydrogen bonds, but also other types of forces including electrostatic interaction and Van der Waal forces. Two important factors for protein stability are burial of hydrophobic residues and steric interactions. A protein folds so that the polar residues are facing the outside and the hydrophobic residues are found inside the core. However, hydrophilic residues found in the protein core are not necessarily destabilizing for the structure, if they enable creating disulfide bridges or hydrogen bonds. (Wang, W., 1999)

4.1.3 Protein aggregation

The most common form of physical instability for proteins is aggregation. Protein aggregates have reduced solubility and activity, modified immunogenicity and are therefore commonly not acceptable in pharmaceuticals. Physical factors affecting aggregation are for instance temperature, ionic strength, vortexing and surface adsorption (Wang, W., 1999)

Aggregation of proteins can happen in many different ways and can either be reversible or irreversible. Irreversible aggregates do neither dissociate upon multiple dilutions, nor in shifts in ionic strength or pH. However, these types of aggregates may dissociate by high pressures (>10^3 bar) or high concentrations of chemical denaturants such as urea, guanidium or ionic surfactants. Furthermore, changes in pH, salt concentration or dramatic changes in protein concentration also affects the aggregation mechanisms. (Amin, S. et al, 2014)

Examples of how aggregation can happen include unfolding of monomeric proteins, reversible self-association of partially unfolded or folded monomers and structural or conformational irreversible reorganization of the oligomer. A mechanism of aggregation formation is described in figure 2 below. (Roberts, C. J. et al., 2011)

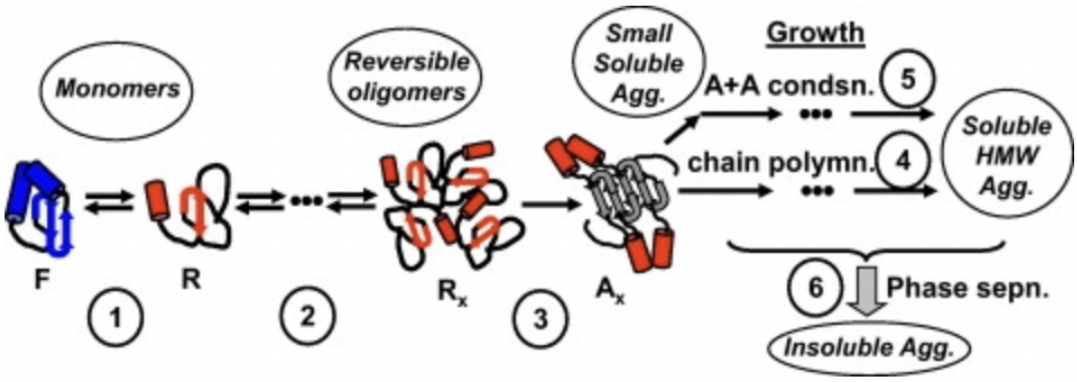

Figure 2. Mechanism of aggregation (Roberts, C. J. et al., 2011).

Aggregates can form by covalent cross-linking (such as di-sulfide bridges) or by strong non-covalent interactions, such as hydrophobic interactions, hydrogen bonds and/or electrostatic interactions. The major driving force is hydrophobic interactions. The most common methods to detect proteins forming aggregates are SE-HPLC and SEC-MALS, which both can be used to detect covalent- and non-covalent bonds. SDS-PAGE and MS are also commonly used for detecting only covalent bonds. (Roberts, C. J. et al., 2011)

4.1.4 Protein degradation & modification

Degradation of proteins can depend on chemical reactions such as deamidation, oxidation, glycation and glycosylation. Research has found that these reactions occur mainly in so-called hot spots in the primary sequence, often close to the amino acids asparagine and aspartic acid at a pH of 4.5-7.5. The most labile motif in the sequence is -Asn-Gly-, followed by -Asn-Ser- and -Asp-Gly-. To a smaller extent -Gln-Gly-, -Asp-Pro- and -Met- are also considered to be such hot-spots. (Wang, W., 1999)

Nowadays, it is common to analyze chemical stability of proteins *in silico*. Advanced computer software as PyMol can be used to predict folding structures and certain areas within a protein especially sensitive towards chemical stress. However, to confirm these predictions, complementary experiments *in vitro* or *in vivo* are needed. (Pramanik, K., et al., 2017)

Deamidation

Deamination is the most common degradation that happens in protein pharmaceuticals. It is most likely to occur in a neutral or alkaline environment. The amino acid that is most susceptible to deamidation is asparagine, followed by glutamine. Furthermore, it has been seen that the residue next to asn on the carboxyl side can have a significant effect on the deamidation rate. To avoid this from happening, the asn residues can be protected in alpha-helical and beta-sheet secondary structures. (Wang, W.,1999)

There have been numerous reports that monoclonal antibodies (mAb's) undergo deamidation. Long storage times of human mAb's result in deamidation along with an increase of other chemical stability problems. In summary, the parameters that have influence on the deamidation rate are the primary sequence, pH (as previously mentioned) and storage temperature. (Manning, M. C., et al. 2010)

Oxidation

Oxidation can either be site specific or non-site specific. Site specific oxidation often occurs at metal binding sites of the protein and is governed by reactive oxygen species. The non-site specific oxidation on the other hand, occurs upon light exposure. The thiol-groups found in the amino acids methionine and cysteine are the most susceptible to oxidation and other residues that potentially can be oxidized include histidine, tryptophan and tyrosine. Factors affecting oxidation are the position of the residue, but also the pH of the formulation as it changes the oxidation potential. (Wang, W., 1999)

Glycation & Glycosylation of proteins

Glycosylation is a post-translational process where carbohydrates can be added to proteins and lipids by enzymes. Glycation on the other hand, is a non-enzymatic reaction, but in the same way glucose or other types of carbohydrates are added onto proteins, lipids and DNA. Another difference is that glycation is an irreversible- and concentration-dependent process. Glycations mainly occur between lysine side chains, as seen in the figure 3 below. (Le Basle, Y., et al. 2020)

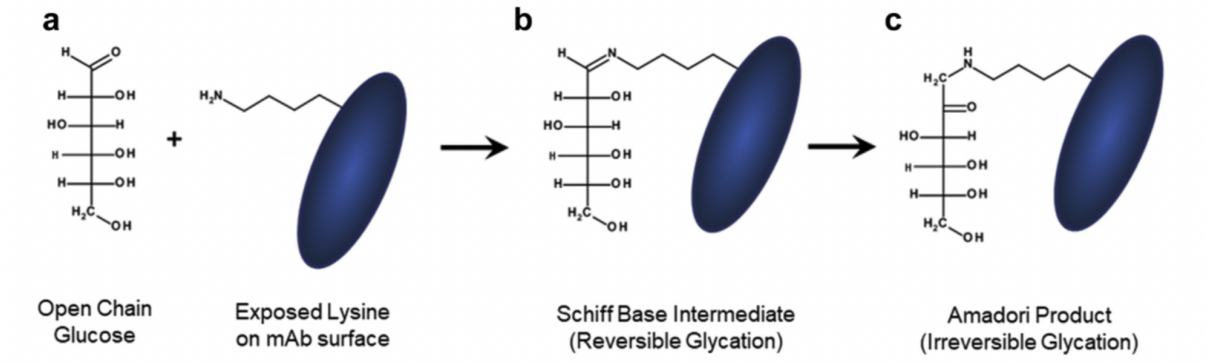

Figure 3. An irreversible glycation reaction between a glucose and a lysine side chain on a monoclonal antibody (mAb) (Le Basle, Y., et al. 2020).

Research has shown that buffers can force glycation in different ways, which can be important since both glycation and glycosylation can increase the conformational stability of proteins to protect them from denaturation. (Le Basle, Y., et al. 2020)

4.1.5 Thermal denaturation

The underlying principles of structural and conformational stability are based on thermodynamics. Monomers that are prone to form aggregates are called reactive monomers. When the free energy of unfolding (ΔG_{f-u}) increases, the concentration of to form reactive monomers from non-reactive folded monomers decreases which in turn leads to a lower rate of aggregation. There are many parameters determining ΔG_{f-u}, and one of high importance is temperature. A commonly used approximation is that in the point where $\Delta G_{f-u} = 0$ for a given folding-unfolding transition, is the melting of the temperature, called T_m. (Roberts, C. J. et al., 2011). This is the point where 50% of the protein molecules are unfolded. Normally, protein thermal denaturation will appear in a temperature range between 40- 60°C. Proteins may have two or more T_m's, and in between these, a stable intermediate. Different T_m's often correspond to different domains of the protein and are common to see in multimeric, chimeric and modular proteins. An example of this is seen in the chimeric protein toxin sCD4-PE40, that consists of a T-cell binding domain (CD4) and a cytotoxic domain (PE-40) where each component has its own transition temperature. (Wang, W., 1999)

4.1.6 Stress and protein instability

The production of a pharmaceutical protein consists of many different steps, all the way from formulation, filtration, shipping, packaging to storage and finally distribution. During these steps, the protein may be exposed to different types of stresses that can damage its structure and function. Examples of stresses could be agitation, temperature, light exposure or oxidation. Because of these risks, it is important to expose the drug product towards these hazards during product development. In this way restraint strategies can be developed to ensure that protein stability can be maintained all throughout the formulation production. (Yang, M., 2015)

Exposing the protein to shear stresses such as stirring, pumping and centrifugation may cause damage to especially high weight proteins, resulting in denaturation and inactivation of the protein. (Elias, C B & Joshi,

J B, 1998). Other types of physical stresses can be changes in temperature and freeze/thaw (FT) stress, which also can induce protein instability. (Wöll A K & Hubbuch J, 2020)

4.2 The human immune system

The immune system, our own barrier against infections to fight diseases, is based on white blood cells - the organs and tissues of the lymph system. It can be divided into two parts; the nonspecific-, also referred to as the innate immune system, and the specific- called the adaptive immune system. The adaptive immune system is built up over time as the body is exposed to different bacteria, viruses and other harmful substances. (Ziessman, H. A., O'Malley, J. P., & Thrall, J. H., 2006). Some of the main components of the immune system are described more in detail below.

Leukocytes

Leukocytes is a collective name for white blood cells and lymphocytes are a type of leukocytes that are made in the bone marrow. Lymphocytes belong to the adaptive immune system. Lymphocytes can be divided into three different cell types; antibody-producing B-cells and T-cells recognizing compounds the body previously has been exposed to and NK-cells, destroying foreign cells entering the body. (Ziessman, H. A., O'Malley, J. P., & Thrall, J. H., 2006)

T-cells

T-cells play a key role in the immune system, specifically during the elimination of foreign substances. The T-cells involved in these processes are CD4 helper T-cells and CD8 cytotoxic T-cells, which both also contain the co-receptor CD3. (News Medical Life Sciences, 2020)

The T-cells circulate in the blood until they find their specific antigen. Upon binding, they can either be targeting infectious diseases or be involved in responses against allergens and tumors (News Medical Life Sciences, 2020). The antigens are presented on so-called APCs (antigen-presenting cells), which for instance can be dendritic cells or macrophages, by the aid of a MHC (major histocompatibility complex) (Hack Dentistry, 2017). MHC binds to the recognition site on the T-cell which is the TCR (T-cell receptor) (Hack Dentistry, 2017). The TCR will not be produced if the CD3 co-receptor proteins are not expressed on the T-cell (Hack Dentistry, 2017). The different components described and how they are connected can be seen in figure 4 below.

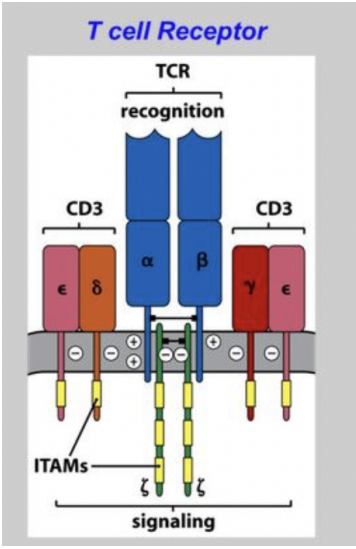

Figure 4. TCR recognition site and CD3 co-receptor of a T-cell (Immunology, 2016).

B-cells; Antibodies & Antigens

The B-cells of the adaptive immune system are responsible for producing antibodies and recognizing and eliminating specific pathogens such as viruses, bacteria, fungi or parasites (Life Science, 2020). Antibodies are proteins in the shape of a Y that search the body for enemies and mark them for destruction. Another name for antibodies is immunoglobulins (Ig). In total, there are 5 variations of Ig's, but all of them have the same Y-shape. They are called IgG, IgM, IgA, IgD and IgE. (Mauri, C., & Bosma, A., 2012)

In figure 5 below a schematic illustration of an antibody is shown, composed of two heavy chains (blue) and two light chains (pink). Both the heavy and light chains are composed of a variable region and a constant region. At the very ends of the two arms on the top of the antibody, are the single chain variable fragments, scFv, where antigens bind specifically to a complementary structure found on the variable region of an antigen. (Mauri, C., & Bosma, A., 2012)

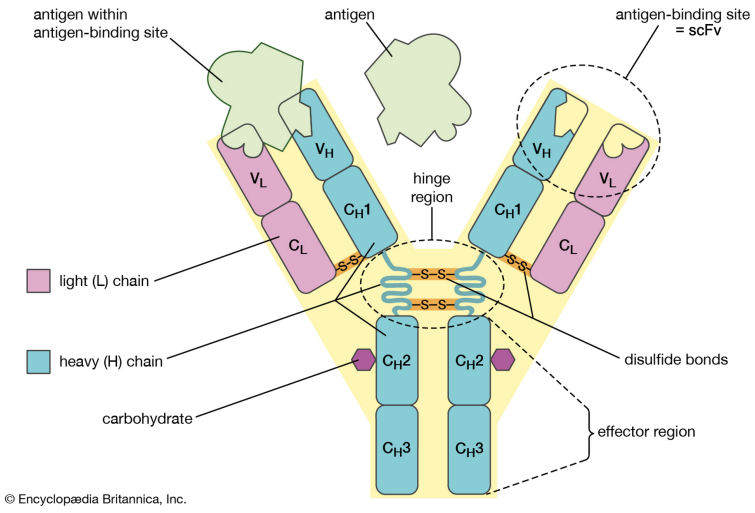

Figure 5. Antibody composition. V=variable, C=constant, H=heavy, L=light, scFv = single chain variable fragment (2021 Encyclopædia Britannica, Inc., 2021).

Any substance that can cause an immune response (i.e antibody release), are called antigens. Antigens can for instance be molecules or molecular fragments from a virus or bacterium. Antigens contain a specific site on their surfaces called epitopes or antigenic determinants. When an immune response is triggered, antibodies are generated against the antigen to interact and recognize the specific epitope. (News Medical Life Sciences, 2020)

4.3 Cancer Immunotherapy

Cancer immunotherapy is a relatively new, widely used cancer treatment that often is used in combination with surgery, chemotherapy and/or radiation. As indicated by the name, the treatment is simply an aid to the patient's own immune system. In addition, cancer immunotherapy is a biological treatment, meaning that the substances that are used originate from living organisms. (National Cancer Institute, 2019)

In some cases, cancer tumors contain tumor-infiltrating lymphocytes (TILs), that facilitates the recognition of the tumor and thereby helps the patient's immune system to fight the cancer on its own. However, this is unfortunately not the case for all cancer types. Cancer cells have developed strategies to trick our immune cells making it difficult for patients to self-recover from the disease. These strategies include genetic changes to stay hidden for the immune system, surface proteins that downregulate the effect of the immune cells and altering the environment around the tumor so that healthy cells start working in collaboration with the tumor. With the aid of cancer immunotherapy, the immune system can overcome these tricks and defeat cancer. (National Cancer Institute, 2019)

BiTEs

There are different variants of cancer immunotherapy and one type is called bispecific T-cell engagers, or BiTEs. BiTEs are bispecific molecules constructed from the scFv of two different antibodies, one binding CD3 on a T-cell (aCD3) and another one binding an antigen exposed on the surface on the target cancer cell. The two scFv's are connected to each other by an artificial flexible linker. This construct allows the body's own immune cells to activate and come in close contact with the tumor cells so they can be defeated, see figure 6 below. (Huehls, A. M et al., 2015, March 19)

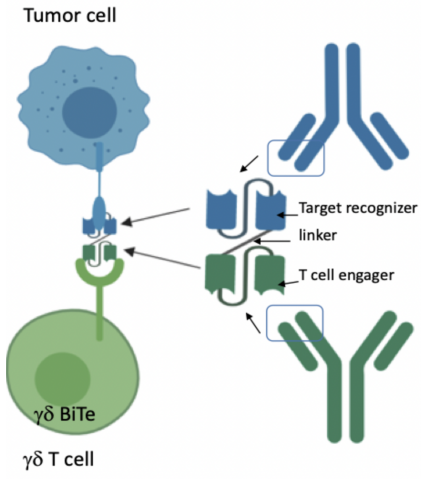

Figure 6. Bispecific T-cell engagers (biTEs), structure and function (Oncobites, 2019).

4.4 Background of rVAR2-aCD3

The idea behind using the rVAR2-aCD3 protein for immunotherapy targeting cancer, was first introduced by Professor Ali Salanti who was developing malaria vaccines for pregnant women in Africa. (University of Copenhagen, 2020)

Pregnancy associated malaria

Malaria infected mosquitoes are one of the main causes of death in many countries across the world. A specific type of parasite transferring malaria is the *Plasmodium falciparum* species, that selectively infects pregnant women. (Clausen, T. M. et al., 2012)

In 2003, Dr. Salanti identified the VAR2CSA protein that was being expressed on the malaria infected red blood cells found in the placenta of malaria infected pregnant women. In the blood stage of a malaria infection, the parasite enters the red blood cells. However, when the red blood cells reach the spleen, the parasite is in risk of being destroyed. Hence, VAR2CSA proteins are expressed on the surface of the red blood cells (figure 7a and 7b) allowing them to attach the sugar structures, chondroitin sulfate proteoglycans (CS), in the placenta of the pregnant woman. If the red blood cells can stay attached to the placenta, they bypass spleen mediated destruction, which in turns lead to a prolonged infection. (University of Copenhagen, 2020)

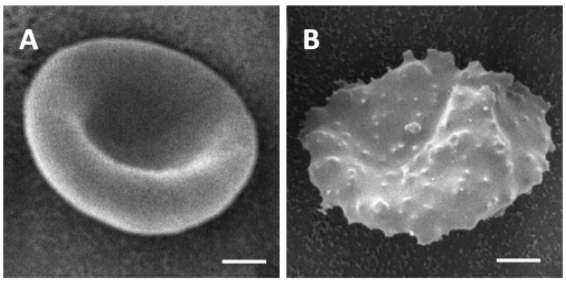

Figure 7a & 7b. Healthy red blood cell (to the left) and red blood cell expressing VAR2CSA on the surface after malaria infection (to the right). (Hayakawa, E. H., & Matsuoka, H., 2016)

Figure 8 below shows a schematic over the connection between the CS on the placental cells and the VAR2CSA protein expressed on the malaria infected red blood cells.

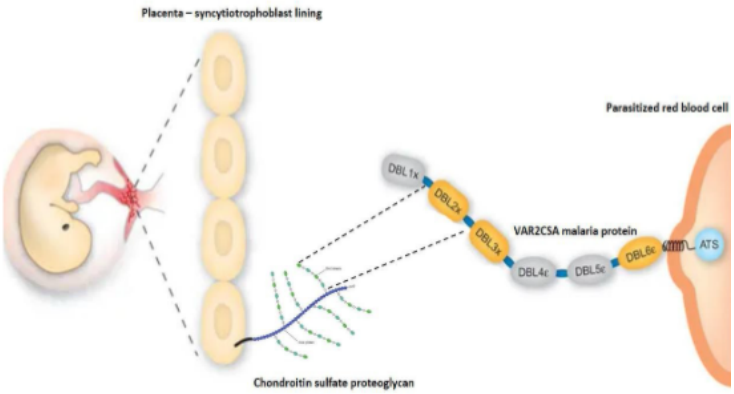

Figure 8. VAR2CSA protein expressed on the malaria infected red blood cells binding to chondroitin sulfate proteoglycans on the placenta of a pregnant woman. (Hayakawa, E. H., & Matsuoka, H., 2016)

VAR2CSA structure & binding

The expression of the surface proteins enabling the connection between the infected red blood cells and the placental organ is encoded by so-called var-genes, naturally found in the genome of the parasite *Plasmodium falciparum.* Amongst the different proteins these var-genes code for, the transmembrane protein VAR2CSA of 350kDa has shown to be the most important for binding. In figure 9 below, a cryo-EM structure of VAR2CSA can be seen, showing the minimal binding region that is found within the core region of the protein. (Higgins, M. K., 2008)

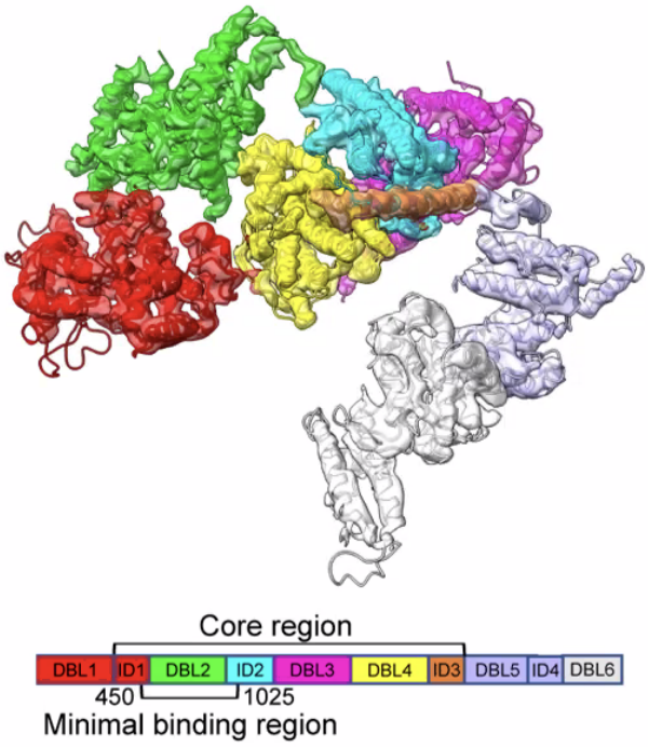

Figure 9. Cryo-EM structure of VAR2CSA protein, showing the minimal binding region found within the core region of the protein (Higgins, M. K., 2008).

In figure 10 below, the different domains of the VAR2CSA transmembrane protein are seen. FV2, is representing the full length of the VAR2CSA protein, consisting of 6 DBL (duffy binding-like) domains. To find the minimal binding region, FV2 was truncated and combined in different ways, seen as the following proteins on the list in figure 10. These different combinations are all referred to as recombinant VAR2 or rVAR2. Their respective binding affinity (Kd) is seen to the right in the figure, where a low number represents high affinity. However, the exact binding mechanism is still unknown to researchers today. (Clausen, T. M. et al., 2012)

Protein	Minimal Binding Region										K_D (nM)
	NTS	DBL1X	ID1	DBL2X	ID2a	ID2b	DBL3X	DBL4ε	DBL5ε	DBL6ε	
FV2		DBL1X	ID1	DBL2X	ID2a	ID2b	DBL3X	DBL4ε	DBL5ε	DBL6ε	5.2
DBL1X-ID2b		DBL1X	ID1	DBL2X	ID2a	ID2b					1.5
DBL1X-ID2a		DBL1X	ID1	DBL2X	ID2a						8.0
ID1-ID2a			ID1	DBL2X	ID2a						7.6
ID1-DBL2Xb			ID1	DBL2X							21.8
DBL1X-DBL2Xa		DBL1X	ID1	DBL2X							N/A[a]
ID1-DBL2Xa			ID1	DBL2X							N/A[a]

[a]Kinetic fit could not be optained due to a lack of binding to CSPG

Figure 10. Regions of the VAR2CSA protein. FV2 is the full-length protein, followed by different truncated and combined versions of rVAR2. (Clausen, T. M. et al., 2012)

Targeting cancer: rVAR2-aCD3

During his work, Dr. Salanti discovered that a carbohydrate structure similar to the placental expressed, chondroitin sulfate A (CSA), was also found on the vast majority of cancer cells and tumors, as shown in figure 11 below (VAR2 Pharmaceuticals, 2020). One can wonder why it is that the placenta has similar sugar structures on its surface as cancer cells. It turns out that many properties characterizing cancer cells are shared with properties of the placental organ, such as unusually rapid growth and angiogenesis promotion to allow a flow of nutrients through the bloodstream to a growing fetus. (Salanti, A., 2015)

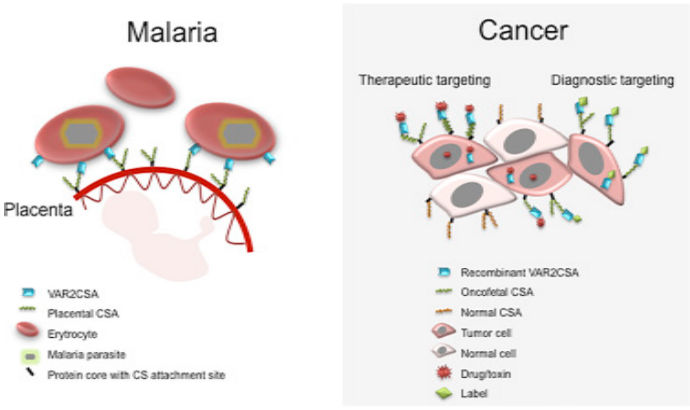

Figure 11. Similarities in sugar structures and proteins found on the placenta in a malaria infected pregnant woman and on cancer cells (Salanti, A., 2015).

Based on this research, an idea started to form to use a protein with VAR2 in immunotherapy for cancer treatment. Today, the research team has discovered that recombinant VAR2, rVAR2, also binds specifically to CSA on human cancer cells *in vitro* and mouse models *in vivo*. As yet, the researchers have not retrieved any data acknowledging that the rVAR2-aCD3 binds any other cells than cancer cells in the body. (Nordmaj, M. A. et al., 2021). The protein can be seen in figure 12 below.

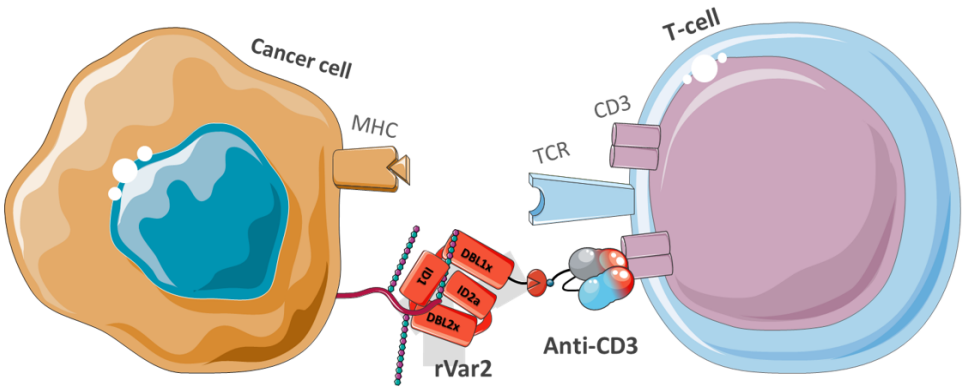

Figure 12. Schematic over the rVAR2-aCD3 anchored to a cancer cell and a T-cell (VAR2 pharmaceuticals, 2020).

The schematic seen in figure 12 above, shows how the rVAR2 binds specifically to the surface of cancer cells. In addition, to activate the patient's own immune system (T-cells), a linker that attaches rVAR2 to the single chain variable fragment (scFv) of aCD3 has been added to the protein that enables binding to the surface of T-cells. This monomer is thought to be used as a future drug for cancer treatment.
As mentioned previously, the MHC found on the cancer cells is usually blocked, hindering the T-cells from finding the cancer cells. To come around this issue, rVAR2-aCD3 can create a new link between the cancer cells and the T-cells. The VAR2 protein binds to CSA which is overexpressed on the surface of the cancer cells and aCD3 binds the CD3 co-receptor found on the T-cells. In this way, the rVAR2-aCD3 works as a "flag" and can activate the T-cells in the body. (National cancer Institute, 2019). The concept has shown promising results in mice and will hopefully continue to phase I clinical trials in the near future. (Nordmaj, M. A. et al., 2021)

The type of cancer immunotherapy the company VAR2 Pharmaceuticals is using is a bispecific molecule, and is in that way similar to BiTEs, that was mentioned previously. What differs between the two therapies, is that in VAR2 Pharmaceuticals product, the scFv of aCD3 is not connected to another antibody's scFv, but to the protein rVAR2, creating the fused protein rVAR2-aCD3.

Currently, the protein is produced in baculovirus transfected insect cells. During the production, the protein undergoes post translational modifications such as N-glycosylation. This modification can increase protein folding and stability and can also protect against proteolysis. (Harrison, R. L., & Jarvis, D. L, 2006). However, if the glycosylation is desired or not for therapeutic usage in the rVAR2-aCD3 protein, is not known.

rVAR2 together with the linker have a molecular size of 70kDa (GenBank, 2009) and the scFv of aCD3 has a size of 27kDa (Kipriyanov, S. M et al., 1997) making up to the total protein size of 97kDa.

4.5 Formulation for protein stabilization

Extrinsic factors that commonly are used to stabilize proteins are sugars, salts and organic osmolytes (Wang, W., 1999). Organic osmolytes are small solutes that are used by cells to maintain the volume inside a cell, as for example amino acids, methylamines, polyols and sugars. The working mechanism of these compounds can be for instance antioxidizing effects or redox balancing. (Yancey, P. H., 2005)

In the following sub headlines different buffers and additives used for protein stabilization are presented. However, it is important to know that all proteins are different and therefore require their own specific mechanisms of stabilization. Thereby, a trial-and-error approach is preferred in protein stabilization studies. (Wang, W., 1999)

4.5.1 Buffers

Due to the different characteristics of proteins, various buffers systems are preferred. The following buffers presented in the table 1 below are commonly used for protein storage.

Table 1. 6 different commonly used buffers for protein formulations.

Buffer	Area of usage	Properties
50mM Citrate	➢ pH range: 3.0-6.2 (Tebu Bio, 2017)	➢ Can be stored up to 3 months in room temperature ➢ Prevents base hydrolysis (AAT Bioquest, 2020)
50mM Sodium acetate	➢ pH range 3.7-5.6 (Tebu Bio, 2017)	➢ Relatively cheap ➢ Can be stored at room temperature for long periods of time (AAT Bioquest, 2020)
50mM MES	➢ pH range 5.5-6.7 (Tebu Bio, 2017) ➢ Biological buffer and commonly used in research (Merck, 2021).	➢ MES = Morpholinoethanesulfonic acid monohydrate (Merck, 2021)
50mM Histidine	➢ pH range 5.0-7.0 (Tebu Bio, 2017) ➢ Suitable for high molecular weight proteins (Chen, B. 2003) ➢ Commonly used buffer for protein formulation, especially in monoclonal antibody formulations (Baek, Y., et al, 2017)	➢ Stabilizes antibodies both in liquid and solid forms ➢ Reduces the viscosity of the solution which is desired for dosage forms ➢ Stabilizes proteins during freezing and thermal stress ➢ Histidine can serve as an antioxidant for reactive oxygen species and can reduce noncovalent interactions of antibodies (Chen, B. 2003)
50mM PBS	➢ pH range 5.8-8.0 (Tebu Bio, 2017) ➢ One of the most widely used buffer solutions (Protocols Online, 2016)	➢ PBS = Phosphate buffered saline (Merck, 2021) ➢ Contains different salts (in 1x PBS): 137mM NaCl, 2.7mM KCl, 10mM Na_2HPO_4, 1.8mM KH_2PO_4 (Merck, 2021) ➢ Properties similar to the isotonic environment inside a human body in terms of buffer osmolarity and ion concentrations ➢ Non-toxic to cells (Protocols Online, 2016) ➢ Can give rise to pH shifts upon crystallization of solutes which can cause problems for the protein stability (Thorat, A.A. & Suryanarayanan, R., 2019)
50mM Tris-HCl	➢ pH range 7.0-9.0 (Sciencing, 2018) ➢ Commonly used buffer for biological applications (Sciencing, 2018)	➢ High solubility in water, making it easy to prepare (Sciencing, 2018)

4.5.2 Tonicity and osmolality

When using additives in a buffer solution for pharmaceuticals to be distributed in the human body, it is important to take tonicity into consideration. Tonicity is the effect a solution may have on cell volume upon osmotic pressure. If the solution causes an increase in cell volume it is called hypotonic, and if it in contrary causes a decrease in cell volume it is said to be hypertonic. Neither of these effects are desired during drug distribution, and it is therefore important to design the buffer solution to be isotonic, meaning that it does not have an impact on the cell volume. (Koeppen, B. M. & Stanton, B. A., 2013)

Osmolality is a measure of solute particles in 1 kg of solution. The intracellular fluid osmolality of red blood cells is 300 mOsm/kg. To avoid inducing osmotic pressure on the cells, the same osmolality should be obtained in a buffer solution for pharmaceuticals to be distributed in the blood. Using sucrose as an additive, this molality would correspond to a concentration of 300 mmol/L, whereas for NaCl the concentration would be 150mmol/L as the salt dissociates into two ions: Na^+ and Cl^-. (Koeppen, B. M. & Stanton, B. A., 2013)

4.5.3 Tonicity providers

To further stabilize proteins in solution, different additives can be used as for instance sugars or salts. The stabilizing effects of sucrose and sodium chloride are presented in the sections below.

Sucrose

Sucrose is a sugar molecule that changes the circular dichroism of the proteins which increases the activation energy of the unfolding process. This small change often increases protein stability (Lee, J. C., & Timasheff, S. N., 1981). In addition, sucrose prevents cold crystallizations especially for high protein concentrations (Hauptmann, A. et al., 2018).

Using sucrose as an additive in histidine buffers has shown to increase the hydrodynamic radius of monoclonal antibodies which can have a potential impact on ultrafiltration or diafiltration processes. (Baek, Y. et al., 2017)

NaCl

Sodium chloride is a commonly used additive in many buffers since it helps mimicking physiological conditions. In addition, it keeps the proteins soluble in a solution. Salts (ion pairs) and charged residues in general, may also affect the denaturation state by increasing the denaturation temperature. Folded proteins are not affected by salts in a significant manner. (Mao, Y. J et al., 2007)

During freezing, the pH and ionic strength in the solution can impact the stability of the compounds. It has been found that dibasic salts can give rise to a decrease in pH while monobasic salts may increase the pH in phosphate buffers. (Van den Berg, L & Rose D, 1959).

4.7 Analytical methods

In table 2 below, an overview of the analytical techniques used is presented as well as their area of usage.

Table 2. Analytical techniques and their respective area of usage.

Technique	Area of usage
NanoDrop	Protein concentration
SE-HPLC	Aggregation, contamination & fragmentation
SDS-PAGE	Aggregation & degradation
Direct ELISA	Binding
FACS	Binding & cell sorting
NanoDSF	Melting temperature
SEC-MALS	Absolute molar mass & size distribution
DLS	Size distribution, hydrodynamic size & polydispersion
MS	Molar mass of degradation segment
NGC	Fractionation of oligomers

In the following sections commonly used analytical techniques for protein stability studies are presented.

SDS-PAGE

Sodium dodecyl sulfate polyacrylamide gel electrophoresis (SDS-PAGE) is a common technique for separating proteins based on size. SDS denatures and adds negative charge to the proteins which makes them electrically mobile. An electrical current is applied across a voltage potential, allowing the proteins to travel through a polyacrylamide gel. Small proteins will move quicker and therefore appear further down in the gel in comparison to larger proteins. Each sample is loaded in two replicas, one where loading dye containing DTT, dithiothreitol, is added (+) that has reducing effect on the protein sample and in the other replica loading dye without DTT is added (-) that instead has a non-reducing effect (Thermofisher, 2020). Furthermore, Coomassie brilliant blue is staining the proteins which enables visualization. By loading one well of the gel with a protein ladder, the different sizes of the proteins easily be distinguished. (Experiment, 2016) To be able to compare two different gels, a common protein of known molecular size can be loaded on both gels. An example of such a protein could be the well-known BSA (bovine serum albumin) that has a molecular size of 66.5 kDa. (Merck, 2021) In figure 13 below, an illustration of an SDS-PAGE set-up is seen.

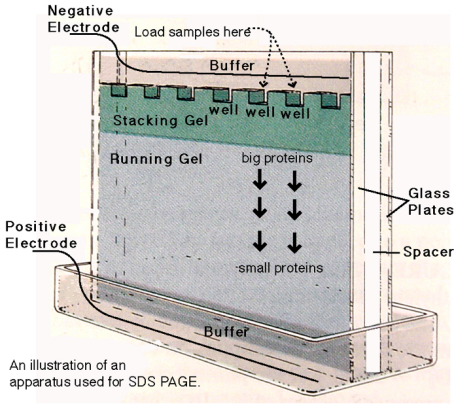

Figure 13. SDS-PAGE set-up (Experiment, 2016).

ELISA

Enzyme-linked immunosorbent assay (ELISA) is a technique used for detecting and quantifying proteins. ELISA is a plate-based assay, where an antigen or antibody has been immobilized to the bottom of the plate that binds enzyme-label-antigens or antibodies. (BOSTER Antibody and ELISA experts, 2020). A substrate is added, which gives rise to a color as it is cleaved. The color is detected and measured by light absorption and further converted into numeric values. There are four different main types of ELISA methods including: direct ELISA, indirect ELISA, sandwich ELISA and competitive ELISA (MBL Life Science, 2017). In figure 14 below, the set-up for direct ELISA is seen.

Figure 14. Direct ELISA set-up (MBL Life Science, 2017).

The set-up for measuring the binding of VAR2 using one plate coated with decorin and one coated with HSPG, is called CSA ELISA. Decorin is an oncofetal chondroitin sulfate glycosaminoglycan chain (ofCS). Many cancer tumors express different proteoglycans modified with ofCS and decorin is therefore considered as a *positive* ligand and the binding of VAR2 is therefore desirable (Reszegi, A. et al., 2020). HSPG is a heparin sulphate proteoglycan which is naturally present on all cells in animals. To prove that VAR2 selectively only binds cancerous tissue and not healthy cells, the HSPG binding is considered a *negative* ligand and its binding to VAR2 is not desirable (Christianson, H. C., & Belting, M., 2014).

A specific enzyme-labeled antibody will bind to the target protein (MBL Life Science, 2017). In the case of VAR2, this enzyme labeled antibody would correspond to the aCD3-VAR2 protein itself with a V5 tag. The V5 tag is a common short peptide tag which can be used for different types of protein detection- and purification methods, such as ELISA (Salanti, A., 2015). In the next step, substrate (TMB-PLUS) is added to each well and lastly, sulphuric acid is added which completes the reaction. The activity of the microplate can be measured by an ELISA reader. The absorbance values are finally converted into numbers that can be plotted as a graph. (MBL Life Science, 2017).

The procedure of a direct CSA ELISA is shown in figure 15 below.

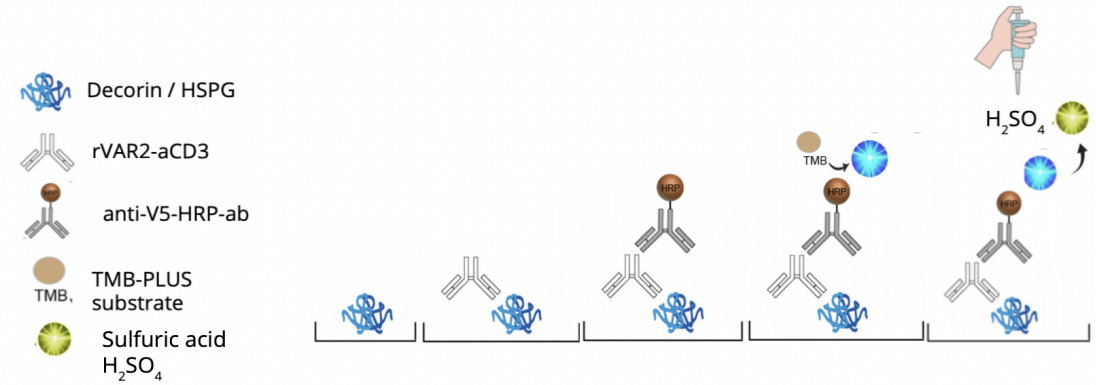

Figure 15. CSA ELISA procedure with a rVAR2-aCD3 protein binding to decorin vs HSPG (Hallberg, F. 2021).

FACS

Fluorescence-activated cell sorting (FACS) is a type of flow cytometry, see figure 16 below. The method can in a rapid and simple way sort single cells in a solution. The sorting is based on the different light scattering and fluorescence characteristics of each individual cell in the sample. A laser beam is used as a light source to produce both the scattered light and the fluorescence, which is then detected by a photodiode or a photomultiplier detector. Finally, the collected signals are converted into electronic signals that can be further analyzed in a computer. (SinoBiological, 2020)

FACS technology is a useful tool for quantitative recording of fluorescent signals of a cell. It can be used for a variety of applications such as immunology, cancer biology and infectious disease monitoring. (SinoBiological, 2020)

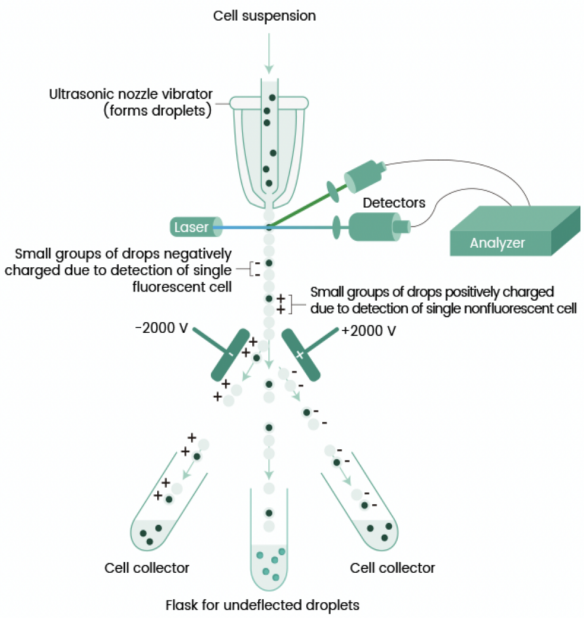

Figure 16. Overview of the scientific FACS instrument including the detector and the analyzing tool. (SinoBiological, 2020).

HPLC

High pressure liquid chromatography (SE-HPLC) is a technique that can separate different compounds in a liquid sample. This technique is widely used in the pharmaceutical industry to perform purity tests of medicines. The set-up consists of different reservoirs containing mobile phases that are mixed in a chamber with the aid of a pump. The mobile phase mixture will then go into a sample injector where the sample enters, and the mixture then enters the HPLC column. Inside the column is the stationary phase containing adsorbent particles, which differ depending on the analysis. As the method is running, the compounds in the mobile phase will interact with the stationary phase. Depending on the differences in physical/chemical properties, such as polarity, the compounds will interact differently with the particles and stick to the column for different amounts of time. Once the substances have run through the column they reach a detector, often a UV/vis detector. UV/vis detectors measure the absorbance of the sample at a specific wavelength, and the signal is then further converted by a computer program visualizing displaying a chromatogram. Due to the different properties of the compounds in the mobile phase and their longer or shorter interaction time with the stationary phase, peaks representing each compound will appear successively after time. Lastly, the column needs to be eluted into the waste canister. (Lösungsfabrik, 2017) In figure 17 below an illustration of the HPLC set-up is seen.

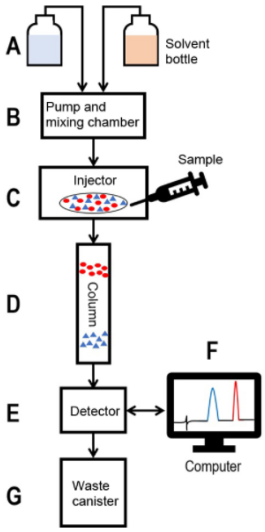

Figure 17. SE-HPLC set-up (Lösungsfabrik, 2017).

Size exclusion chromatography (SE-HPLC) is one type of HPLC, separating compounds by their different sizes. The largest compounds come out first, followed by the smaller in size order. Quantifying aggregations rates is mostly performed by SE-HPLC. (Roberts, C. J. et al., 2011)

NGC

Next generation chromatography, or NGC, is an optimized version of HPLC that often is used in clinical research and for quality controls. In comparison to regular HPLC, the technique is more robust, scalable, flexible and productive. The system is fully automated, has a high throughput and allows for changing settings and parameters along the way as it is running. Furthermore, it contains a fraction collector which enables purification of proteins from a mixed sample. (Bio-Rad, 2021)

NanoDSF

Nano differential scanning fluorimetry, NanoDSF, is used to create melting curves of proteins in solution by measuring the ratio of intrinsic fluorescence between 330nm and 350nm as the temperature is increased (2 bind molecular interactions, 2020). The intrinsic fluorescence originates from Tyrosine, Tryptophan and Phenyl-Alanine residues containing aromatic side chains. The apparent melting temperature (T_m) of when half the protein has unfolded can be determined by the relation between the used temperature gradient and the measured intrinsic fluorescence. The T_m is marked with a dashed line in the melting curves and the dotted lines represent when the unfolding starts, see figure 18 below. (Kwan, T. O. C. et al., 2019) NanoDSF can also give information about cooperative (two-state) folding processes or more complex unfolding transitions, often shown as a first derivative of the melting curve. To summarize, NanoDSF is a fast way to determine the conformational stability of proteins in solution. (Coriolis Pharma, 2020). Illustration from a NanoDSF melting curve can be seen in figure 18 below.

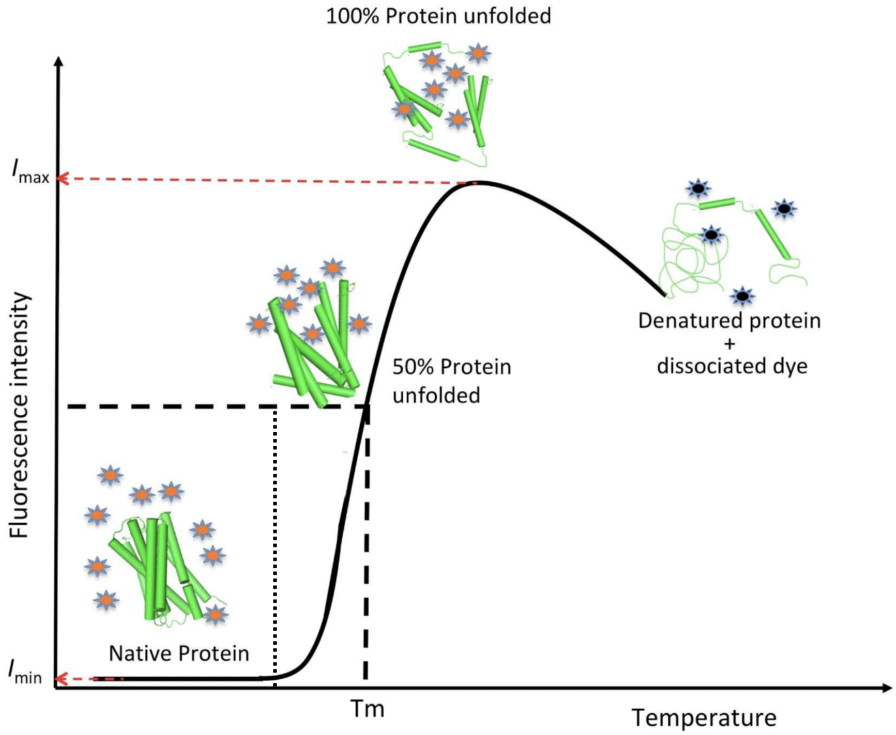

Figure 18. Illustration of a melting curve obtained from a NanoDSF measurement (Kwan, T. O. C. et al., 2019).

NanoDrop

The NanoDrop spectrophotometer is unique in its way, allowing detection at low sample volumes of only a few microliters using the extinction coefficient of the target protein. Furthermore, the retention time is much shorter in comparison to other spectrophotometers. The device detects protein- and nucleic acid concentrations in a wide range of wavelengths (220-750nm) with the aid of a computer software. (Biocompare, 2003)

Filtering method: Desalting columns

The idea behind desalting columns is similar to the principle of size exclusion chromatography, as compounds in a solution are filtered and separated based on their size. The columns consist of matrix beads with pores

allowing small compounds to flow through the column and larger molecules to stay in the top section of the column. The desalting columns are simple to use for purification of for example proteins and nucleic acids from salts and other types of small molecules that can be found in a solution. (Bio-rad, 2020)

DLS

DLS (Dynamic Light Scattering), is a technique used to determine hydrodynamic size and polydispersity in a solution. A monochromatic light beam is passed through the sample and as it reaches the molecules in the solution, the light will be scattered in different directions which is collected by a detector. Based on the Brownian motion of the macromolecules in the solution, a correlation between size (hydrodynamic radius R_H), temperature (T) and solvent viscosity (η) can be calculated, as seen in Stokes law in equation 1 below. (Stetefeld, J., McKenna, S. A., & Patel, T. R., 2016)

Eq.1
$$D = \frac{k_B T}{6\pi\eta R_H}$$

Eq 1. Stokes law. Abbreviations: D = translational diffusion coefficient (m^2/s), k_B = Boltzmann's constant (m^2kg/Ks^2), T = temperature (K), η = viscosity (PaS), R_H = hydrodynamic radius (m). (Paar, A., 2021)

The distribution of the particles in solution can either be monomodal or multimodal. In a multimodal solution all particles are of the same size and in a multimodal solution varying sizes are present. Furthermore, the solution can either be mono- or polydisperse. In a polydisperse system, aggregates of the particles with varying sizes are found, whereas all particles are separated in a monodisperse system. (Wyatt Technology, 2017) The different distributions give rise to different graph-formations, presented in figure 19 below.

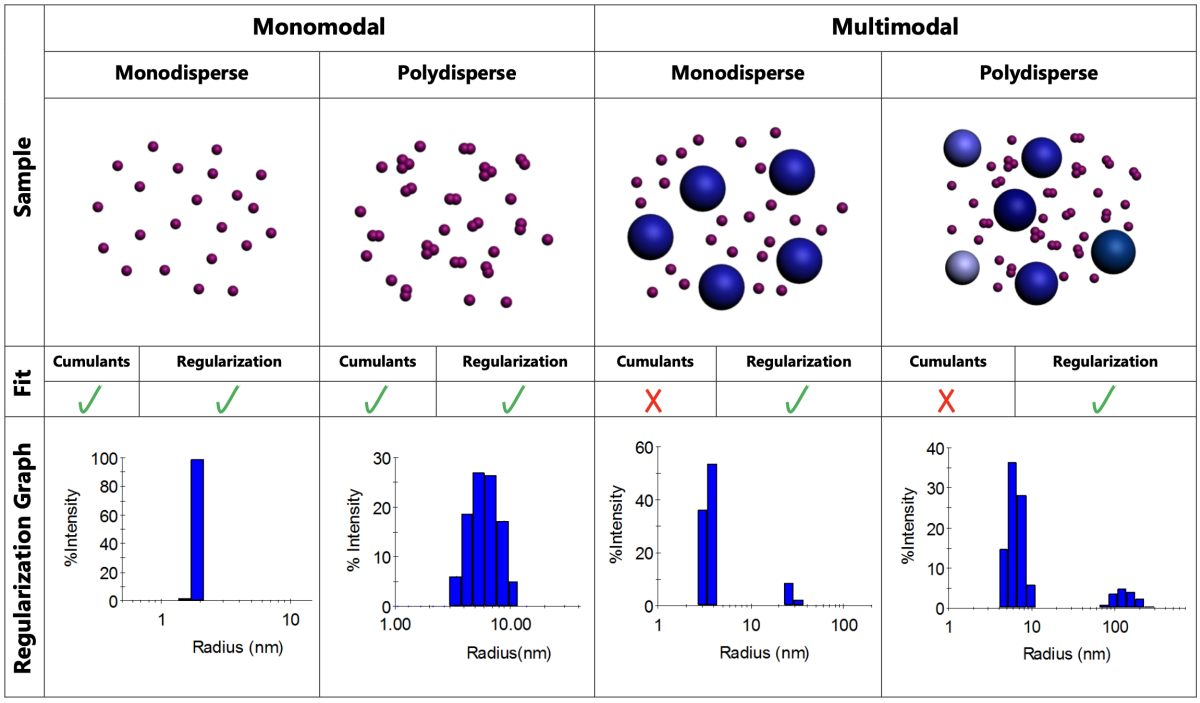

Figure 19. DLS distribution patterns (Wyatt Technology, 2017).

SEC-MALS

Size exclusion chromatography multi angle light scattering is, as intended by the name, a technique that combines SE-chromatography with multi-angle light scattering. The combination allows for determination of the absolute molar mass and the average size of molecules in a solution. The technique can furthermore give information about conformation and conjugation ratio, and by combining the two above mentioned techniques, limitations commonly faced during usage of columns may be overcome. SEC-MALS is commonly used for basic protein and polymer characterization. (Wyatt Technology, 2021)

MS

Mass spectrometry is a technique that measures the mass-to-charge ratio of charged particles. The molecules in solution are converted into ions allowing them to be easily moved and manipulated by external electric and magnetic fields. This enables measuring the mass of particles, chemical structures and basic chemicals found in the solution or within a molecule. The process is based on 5 main steps: vaporization, ionization, acceleration, separation and finally detection. At the end of the procedure the detector converts the collected data to a fragmentation pattern of molecular ions. (MSU Chemistry, 2013)

4.8 Data analysis

Two computer software commonly used in combination with laboratory work are presented below.

SAS JMP

SAS (Analytics Software & Solution) is a computer software package that is used for simulating, reporting and analyzing statistical data. JMP (or "JUMP " as it is often pronounced) is a business unit inside the SAS package, commonly used by scientists, engineers and researchers for visualizing and investigating analytical data. (JMP Statistical discovery from SAS, 2013). In a study like this, the SAS JMP software can be used as a tool for predicting the optimal condition parameters of a protein solution to avoid performing more experiments than necessary.

PyMOL

PyMOL is a computer software within the Python License used to simulate 3D images of small molecules and proteins (PyMOL, 2021).

5. Materials & methods

An overview of the experimental plan is presented in figure 20 below.

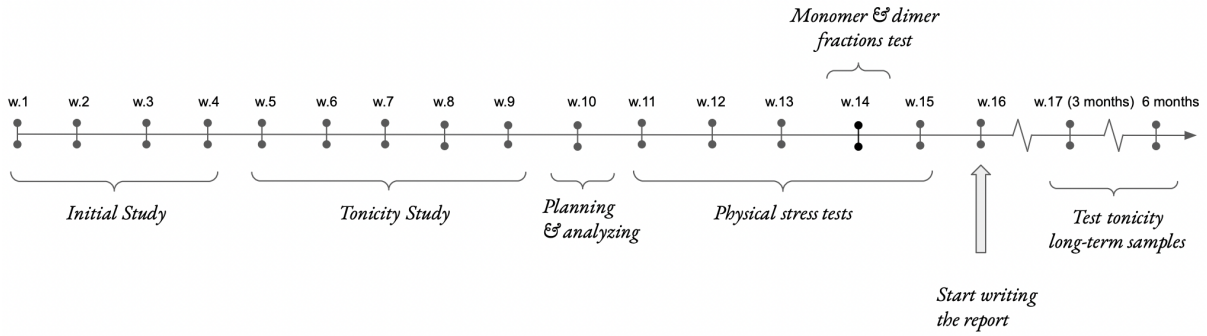

Figure 20. A schematic overview of the experimental plan.

5.1 *In silico* modelling

An *in silico* model of the recombinant VAR2-aCD3 protein was simulated in the open source molecular visualization system called PyMOL. The simulation was performed by the consultancy firm CMCAssist.

5.2 Initial study

The initial study that was performed included preparation of 6 different buffers with pH ranging from 3-8. The buffers and their respective pH can be seen in table 3 below.

Table 3. Buffers used in the initial study with pH ranging from 3-8.

Buffer	Additive	pH range	pH
50 mM citrate	150mM NaCl	3.0-6.2	3.3
50 mM acetate	150mM NaCl	3.6-5.6	4.6
50 mM MES	150mM NaCl	5.5-6.7	6.0
50 mM histidine	150mM NaCl	5.5-7.4	6.0
50 mM PBS	-	5.8-8.0	7.5
50 mM tris-HCl	150mM NaCl	7.0-9.2	8.0

In addition, 150mM NaCl was added to each buffer to stabilize the fusion protein. No extra salt was added to the PBS buffer, since it already contains NaCl. The choices of buffers and salts were made upon literature research and previous studies performed by the company. The fusion protein was desalted and concentrated and then added to each buffer solution. All samples were stored in a 4°C refrigerator and a -80°C freezer

respectively. No aliquots were made, instead the samples were frozen and thawed in between each performed experiment.

The prepared samples were used to get familiar with the analytical techniques and the laboratory and how to interpret stability study results. The analytical methods performed were SDS-PAGE (repeated 3 times), CSA ELISA (repeated 2 times) and NanoDSF. In addition, an SE-HPLC experiment was run on the pure protein sample. The repeated experiments were performed weekly.

Detailed lab protocols for each analytical technique are found in appendix 2.

5.3 Tonicity study

The tonicity study that was performed included preparation of 6 different buffers, 4 with additive salt (NaCl) and 2 with additive sugar (sucrose). The buffers and their respective additive and pH can be seen in table 4 below.

Table 4. Buffers used in the tonicity study with additive salt or sugar.

Buffer	Additive	pH range	pH
50 mM histidine	300mM sucrose	5.5-7.4	6.0
50 mM tris-HCl	300mM sucrose	7.0-9.2	8.0
50 mM MES	150mM NaCl	5.5-6.7	6.0
50 mM histidine	150mM NaCl	5.5-7.4	6.0
50 mM PBS	-	5.8-8.0	7.4
50 mM tris-HCl	150mM NaCl	7.0-9.2	8.0

The choices of buffers were made upon results from the initial study. Sucrose and NaCl were chosen as stabilizers (tonicity providers) based on literature research supporting them being common additives for protein stabilization. The buffers were sterile filtered, and the fusion protein was desalted and transferred into each of the different buffers. Aliquots of 50μL were made of each buffer representing samples for week 0, week 1, week 2, week 3 and week 4 respectively for the tonicity study. In addition, aliquots with larger sample volumes (100μL) to see if precipitates would appear in the samples after storage, and two samples to be saved for longer storage time, 3 months and 6 months respectively, were prepared of each of the buffers. All aliquots had a concentration around 2mg/mL. Information about the proteins, volumes and concentrations are found in appendix 6.1.

The analytical methods performed weekly were SDS-PAGE, CSA ELISA and SE-HPLC. In addition, CD3 ELISA was performed three times (week 1, week 4 and week 12), SEC-MALS was performed once (week 2),

NanoDSF was performed once (week 2), FACS was performed four times (week 2, 3, 4 and 12) and DLS was performed once (week 4).

Detailed lab protocols for each analytical technique are found in appendix 2.

FACS - gating

The FACS analysis was made on purified PBMCs from the same donor in all repeated experiments. Figure 21 below, shows the gating of lymphocytes and single cells that was performed. In addition, the figure shows the negative control peak from a well without protein that the gating resulted in.

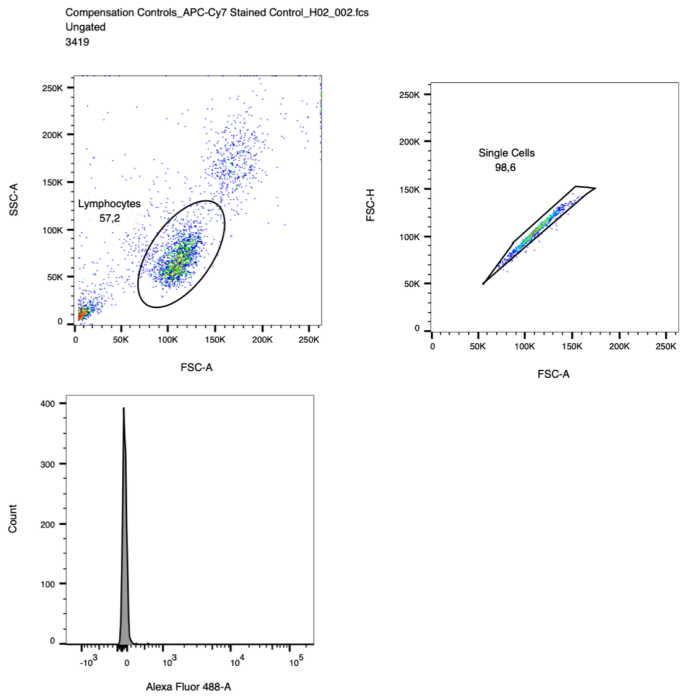

Figure 21. Gating procedure repeated for all samples. Top-left figure: gating for lymphocytes, top right: gating for single cells, bottom figure: negative control peak upon gating.

Furthermore, gating for T-cells (both CD4- and CD8-positive), can be seen in figure 22 below. The positive gating for T-cells was performed and the intensity was measured by an APC fluorophore. The T-cells of interest were further selected by plotting the fluorophores PE-CY7 (CD4 positive) against APC-CY7 (CD8 positive), as seen in the bottom left figure, and the cells of each type could be gated for. The bottom left graph shows the positive peak of the Alexa Fluor 488 fluorophore, binding the VAR2-part of the protein.

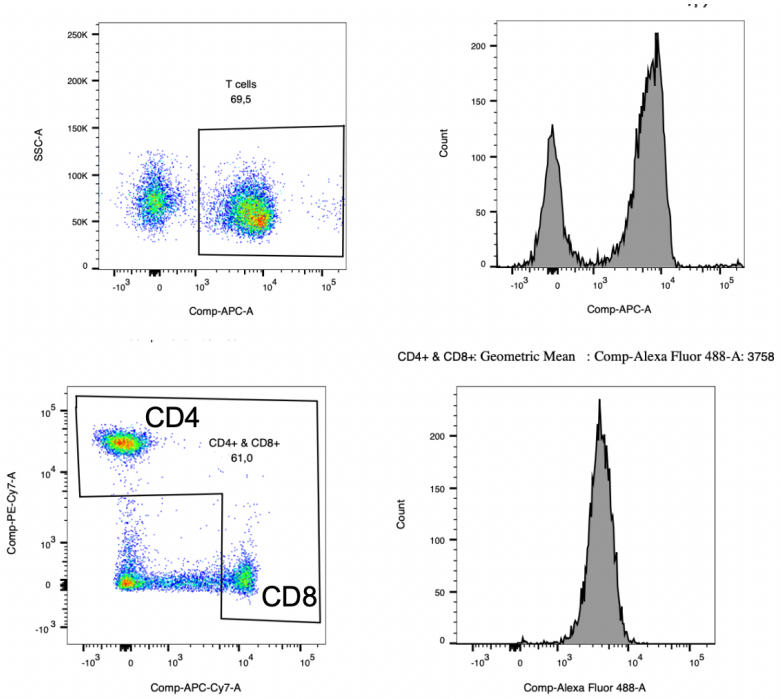

Figure 22. Gating procedure of CD4- and CD8-positive T-cells. Top left figure: gating of T-cells (APC positive). Top right figure: positive peak (APC binding T-cells - desired) and negative peak (not APC binding T-cells). Bottom right figure: gating of CD4- and CD8 binding T-cells respectively and bottom right figure: positive peak arising from the rVAR2-aCD3 protein upon gating.

The data collected from the performed analytical methods were used in the analytical computer software SAS JMP, presented in the section below.

SAS JMP

The collected data was analyzed in SAS JMP. The inputs were: maximized peak% at 27 minutes from SE-HPLC, maximized band% at 104kDa from SDS-PAGE (DTT+) and minimized Kd values from CSA ELISA with decorin. The chosen importance for each parameter was set to 33%. The outputs were pH (6-8) and storage temperature (4°C and -80°C).

5.4 Stress study

In preparation of the stress studies, a pre-study was performed to gain understanding of how stressed the protein would become when being stored at room temperature. One 100µL sample of 1mg/mL protein in PBS buffer was left in a dark incubation hood at 25°C. The sample was analyzed by SDS-PAGE and SE-HPLC after 0, 3, 6, 11 and respectively 19 days to observe changes in stability. The results from the pre-study can be found in appendix 5.

After analyzing the results of the pre-study, three different physical stress studies were performed using three different buffers. The buffers were prepared in the tonicity study and then sterile filtered once more before the starting the stress study. The buffers and their respective additive and pH can be seen in table 5 below.

Table 5. Buffers used for stress tests 1, 2 & 3 with different pH and additives.

Buffer	Additive	pH range	pH
50mM histidine	150mM NaCl	5.5-7.4	6.0
50mM PBS	-	5.8-8.0	7.4
50mM tris-HCl	300mM sucrose	7.0-9.2	8.0

The choices of buffers were made upon results from the tonicity study. Larger aliquots (>100µL) were prepared for the stress study in comparison to the previous studies to facilitate precipitation observations. All aliquots had a concentration around 1mg/mL. Exact aliquot volumes and concentrations are found in appendix 6.1 and 7.2.

The three stress tests that were performed are presented in table 6 below.

Table 6. Three physical stress studies examining changes in stability due to storage in room temperature, shear stress, respectively freezing and thawing.

Stress study	Type of stress	Performance	Duration
1	Storage at room temperature	Samples were left in a dark incubation hood at 25°C	19 days
2	Storage at room temperature + rotation (shear stress)	Samples were left in a dark incubation hood at 25°C and rotated for 30 minutes per day in a blood turner	19 days
3	Freezing and thawing	Samples were stored in a -20°C freezer. Each day, the samples were taken out from the freezer, thawed by hand and left in a dark incubation hood at 25°C for 3 hours before being frozen again. No snap freezing was performed.	6 freeze-thawing cycles

The analytical methods performed weekly were SDS-PAGE, CSA ELISA and SE-HPLC. In addition, MS was performed on two bands appearing on the SDS-PAGE gel (see result section). Furthermore, NGC was performed to fractionate the monomers and dimers of the samples and SDS-PAGE, SE-HPLC and ELISA were performed on the fractionated proteins. After the five weeks NanoDSF was performed on histidine NaCl and tris-HCl sucrose samples from stress study 1 and 2.

Detailed lab protocols for each analytical technique are found in appendix 2.

6. Results

In the following sections the results are presented.

6.1 *In silico* modelling

A three-dimensional structure of the human rVAR2-aCD3 fusion protein simulated *in silico* by the company CMC Assist, is seen in figure 23 below.

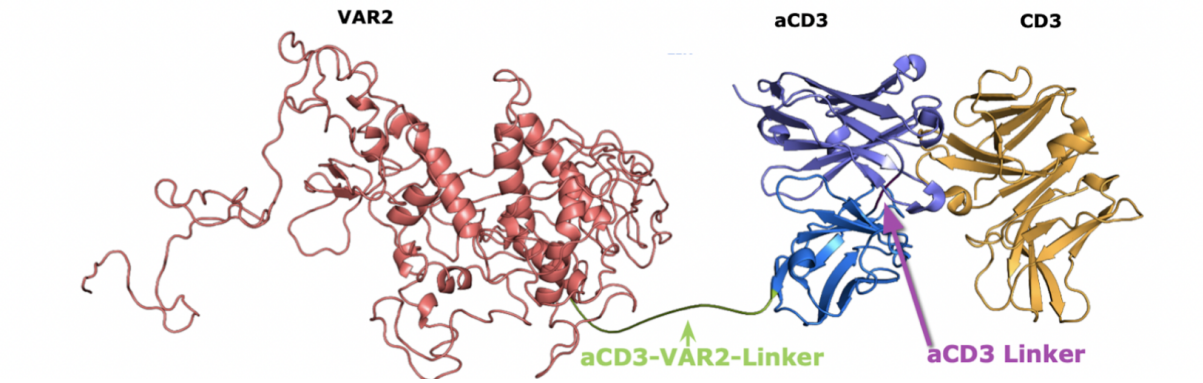

Figure 23. Simulated 3D structure of the human rVAR2-aCD3 fusion protein (Persson, M., Strøm-Hansen, A., 2021).

It is seen in the figure that the VAR2 part of the protein, marked in red, mainly consists of alpha helices whereas the scFv of the aCD3 antibody mainly consist of beta sheets, marked in blue. In between the VAR2 protein and the aCD3 antibody is an artificially made linker, marked in green in figure 23. As only one scFv of the full aCD3 antibody is used in the complex, there is also a linker between the part of the scFv originating from the heavy chain, marked in purple, connected to the part originating from the light chain, marked in blue.

In the amino acid maps found in appendices 1.1 and 1.2, hotspots in the aCD3-part of the protein more prone to chemical degradation caused by deamidation, oxidation and light-induced oxidation are presented. The areas of highest interest are the CDRs (Complementarity-determining regions) which are important to binding.

In the CDRH2 region of the scFv's heavy chain, three asparagine amino acids are found which are potential sites for deamidation. Asparagine is also found in the CD3-L1 and CDR-L3 of the light chain. Also, in the CDRL-3 region of the scFv's light chain, two glutamines are found which also are potential sites of deamidation. One glutamine is also found in the CHRH2 part of the heavy chain. The CDRL-3 furthermore contains a tryptophan which is prone to light-induced oxidation. Lastly, methionine is found both in the CDRH1 of the heavy chain and CHR-L1 of the light chain, which is prone to oxidation.

6.2 Initial study

In the following section, the results from the initial study performed over 3 weeks are presented.

NanoDSF

The results from the NanoDSF are seen in figure 24 below. The melting curves of the rVAR2-aCD3 protein in the 6 different buffers are shown in the top graph and in the graph below, the first derivative of the melting curves is presented.

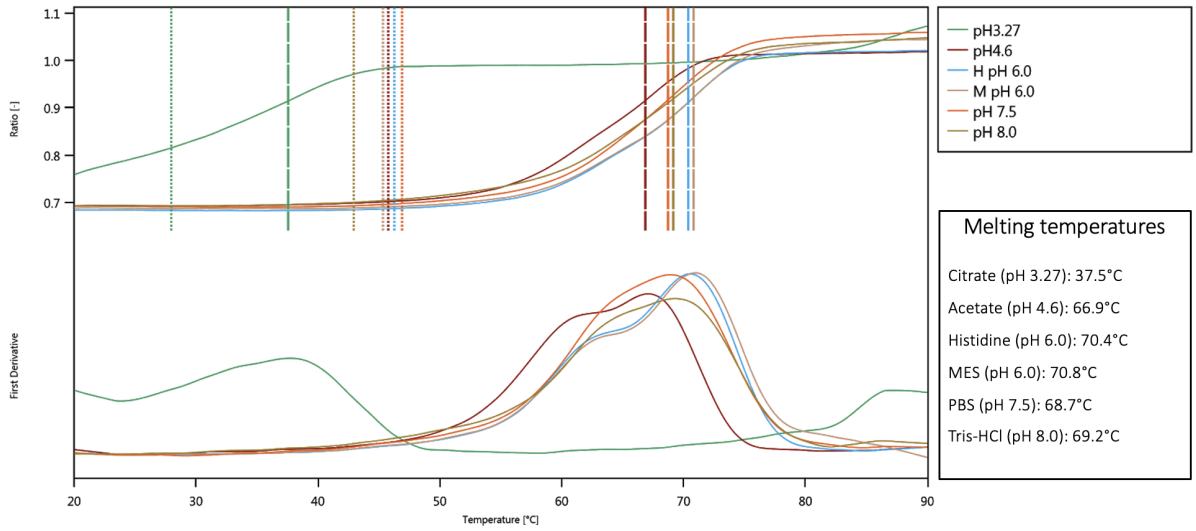

Figure 24. NanoDSF results for 6 different buffers ranging in pH between 3-8.

In the first derivative (bottom curve in figure 24 above), two different melting curve patterns can be observed, either with one single peak or two peaks. As presented in table 7 below, the buffers with a pH >7 had one peak and buffers with pH <7 had two peaks. The citrate buffer does not follow this pattern and has therefore been excluded from the table.

Table 7. Curve patterns of the different buffers observed by NanoDSF and their pH dependence

Buffer	Storing temperature	pH	One peak	Two peaks
Citrate NaCl	4°C	3.3		
Acetate NaCl	4°C	4.6		x
MES NaCl	4°C	6.0		x
His NaCl	4°C	6.0		x
PBS	4°C	7.5	x	
Tris NaCl	4°C	8.0	x	

SDS-PAGE

The results from the SDS-PAGE from week 0 are seen in figure 25 below. Further SDS-PAGE gels from weeks 1 and 2, stored in 4°C and -80°C respectively, can be found in appendices 3.1.1 and 3.1.2.

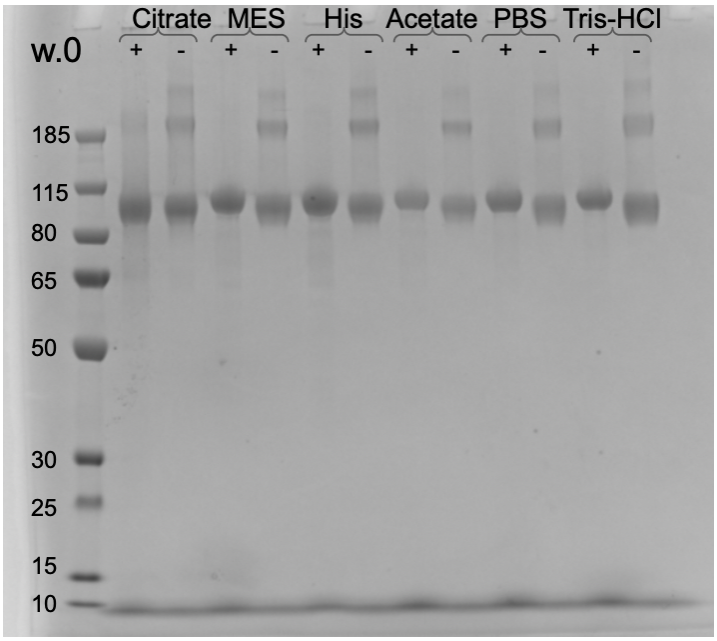

Figure 25. SDS-PAGE gel from week 0. Histidine buffer is abbreviated His. The unit of the protein ladder seen to the left is kDa.

In the gel seen in figure 25above, a clear band is seen around 104kDa in the wells loaded with DTT dye (+) and around 100 kDa in the wells without DTT (-). In addition, bands at 200kDa and 300kDa are seen in the wells without DTT (-).

In appendices 3.1.1 and 3.1.2 it is seen that new bands had appeared in almost all samples from the week 2 measurement (stored in both 4°C and -80°C) around 65kDa in wells with DTT dye (+) and 55 kDa in wells without DTT (-).

SE-HPLC

The chromatogram from the SE-HPLC that was run on the rVAR2-aCD3 protein in PBS buffer is seen in figure 26 below.

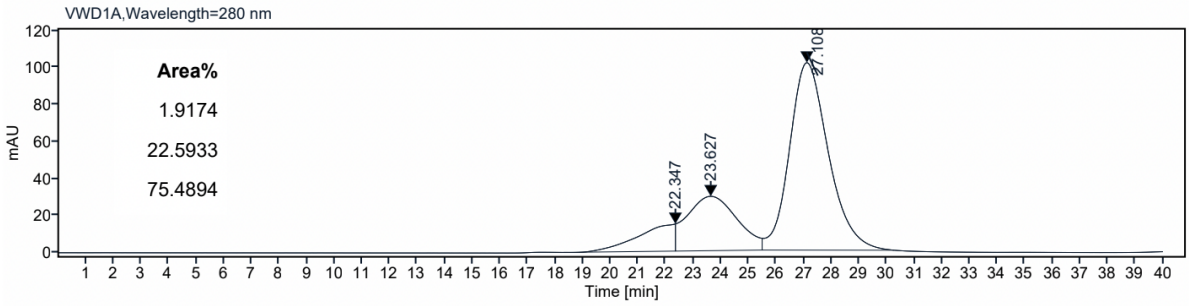

Figure 26. Chromatogram from SE-HPLC of rVAR2-aCD3 in PBS buffer.

Three peaks are observed at around 27 minutes, 24 minutes and 22.5 minutes, respectively, where the peak at 27 minutes has the highest intensity.

CSA ELISA

The results from CSA ELISA measured week 1, stored in both 4°C and -80°C are seen in figures 27a and 27b below.

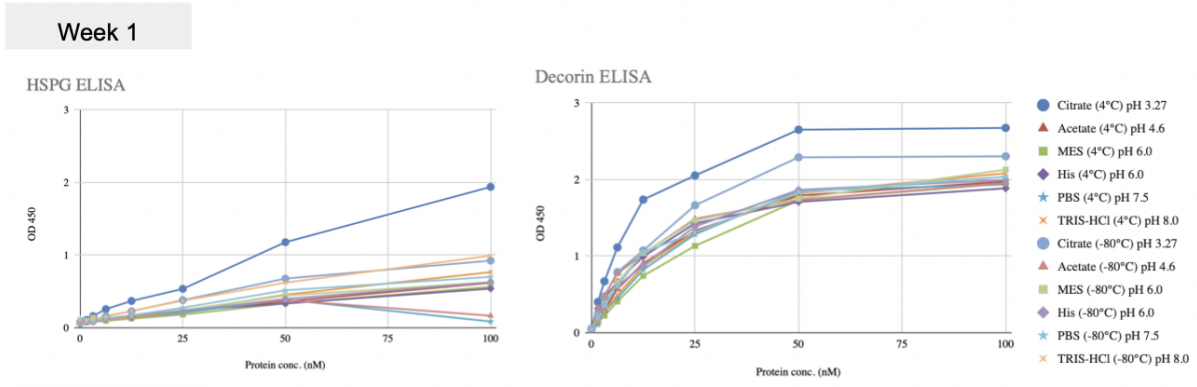

Figure 27a & 27b. Results from CSA ELISA (27a: HSPG binding, 27b: decorin binding) week 1, stored in both 4 °C and -80°C.

In figures 27a and 27b above, an overall higher binding is seen towards decorin and a lower binding is seen towards HSPG. Tris-HCl -80°C has been removed from the decorin ELISA plot due to a protocol error where no substrate was added in the wells, which in turn did not give rise to any fluorescence to be measured.

6.3 Tonicity study

During the preparation of the buffers, there were some troubles with the histidine sucrose buffer. Only around 52% of the intended protein amount was obtained after the desalting and therefore fewer aliquots were prepared of this buffer. The exact aliquot volumes are found in appendices 6.1 and 7.1.

In the following section, the results from the tonicity study performed over 5 weeks are presented.

NanoDSF

The results from the NanoDSF measurement are seen in figure 28 below. The melting curves of the rVAR2-aCD3 protein in the 12 different buffers are shown in the first graph and in the graph below, the first derivative of the melting curves is presented.

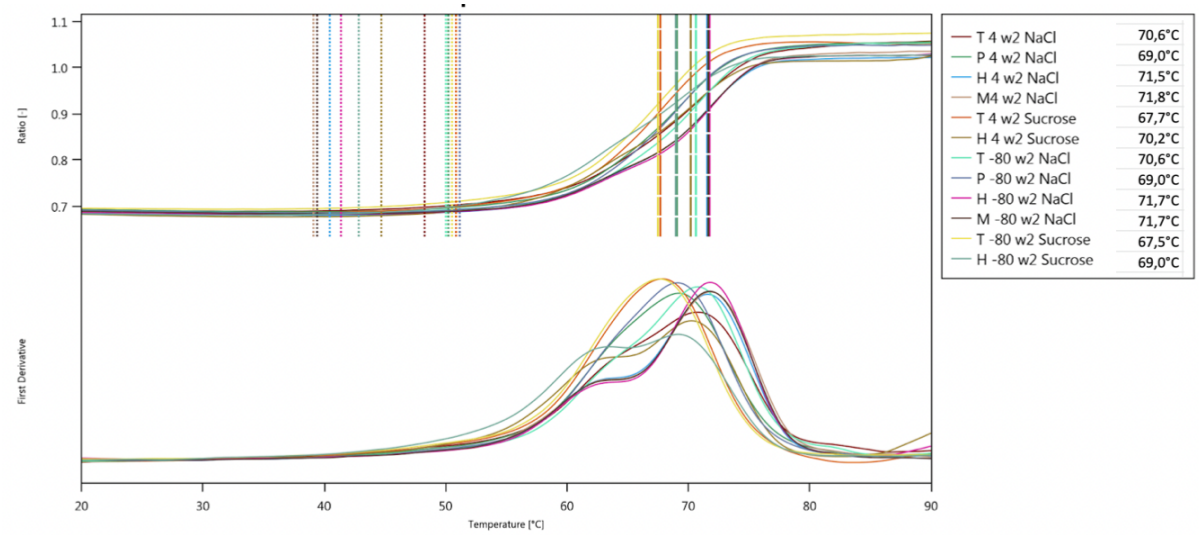

Figure 28. Melting curves obtained from NanoDSF measurement of 12 different buffers ranging in pH from 6-8.

In the first derivative (bottom curve in figure 28 above), two different melting patterns can be observed, either with one single peak or with two peaks. As presented in table 8 below, the buffers with a pH >7 tended to have one peak and buffers with pH <7 had two peaks.

Table 8. Curve patterns of the different buffers observed by NanoDSF and their pH dependence.

Buffer	Storing temperature	pH	One peak	Two peaks
Histidine sucrose	4°C	6		x
Histidine NaCl	4°C	6		x
MES NaCl	4°C	6		x
PBS	4°C	7.4	x	
Tris-HCl sucrose	4°C	8	x	
Tris-HCl NaCl	4°C	8	x	
Histidine sucrose	-80°C	6		x
Histidine NaCl	-80°C	6		x
MES NaCl	-80°C	6		x
PBS	-80°C	7.4	x	
Tris-HCl sucrose	-80°C	8	x	
Tris-HCl NaCl	-80°C	8	x	

SDS-PAGE

The SDS-PAGE gels were analyzed in the computer software ImageQuant, where the molecular weight of the protein represented by the strongest band in the wells loaded with DTT dye (+) could be calculated. Figure 29 shows the result from the tris-HCl buffer with sucrose, stored in 4°C measured week 1 of the tonicity study. This measure is representative for all the buffers over all five weeks.

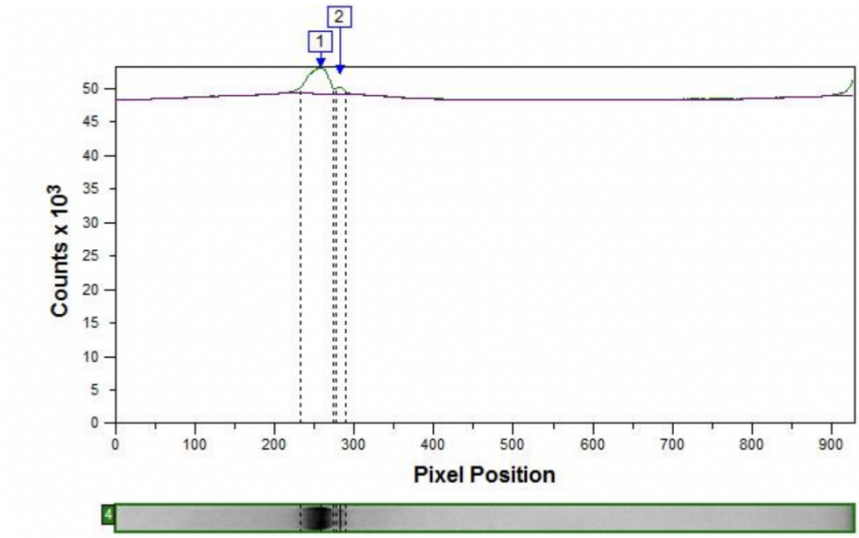

Band Table

Band No	Volume	Vol+BkGnd	Calib Vol(ug)	MW	Rf
1	7414357,89	140709374,00	1,13	104,409	0,278
2	709204,43	42926763,00	0,11	93,842	0,304

Figure 29. Calculated molecular weight of proteins seen in SDS-PAGE gel, in a well loaded with tris-HCl sucrose buffer and DTT dye (+) stored in 4°C measured week 1. The size was calculated using ImageQuant.

As marked in red in figure 29 above, the program calculated the protein to have a molecular weight around 104kDa.

The results from the SDS-PAGE measurements from weeks 0, 4 and 12 stored in 4°C and -80°C respectively, are seen in figure 30 below. Further SDS-PAGE gels from weeks 1, 2 and 3 stored in 4°C and -80°C respectively, can be found in appendix 4.1.2.

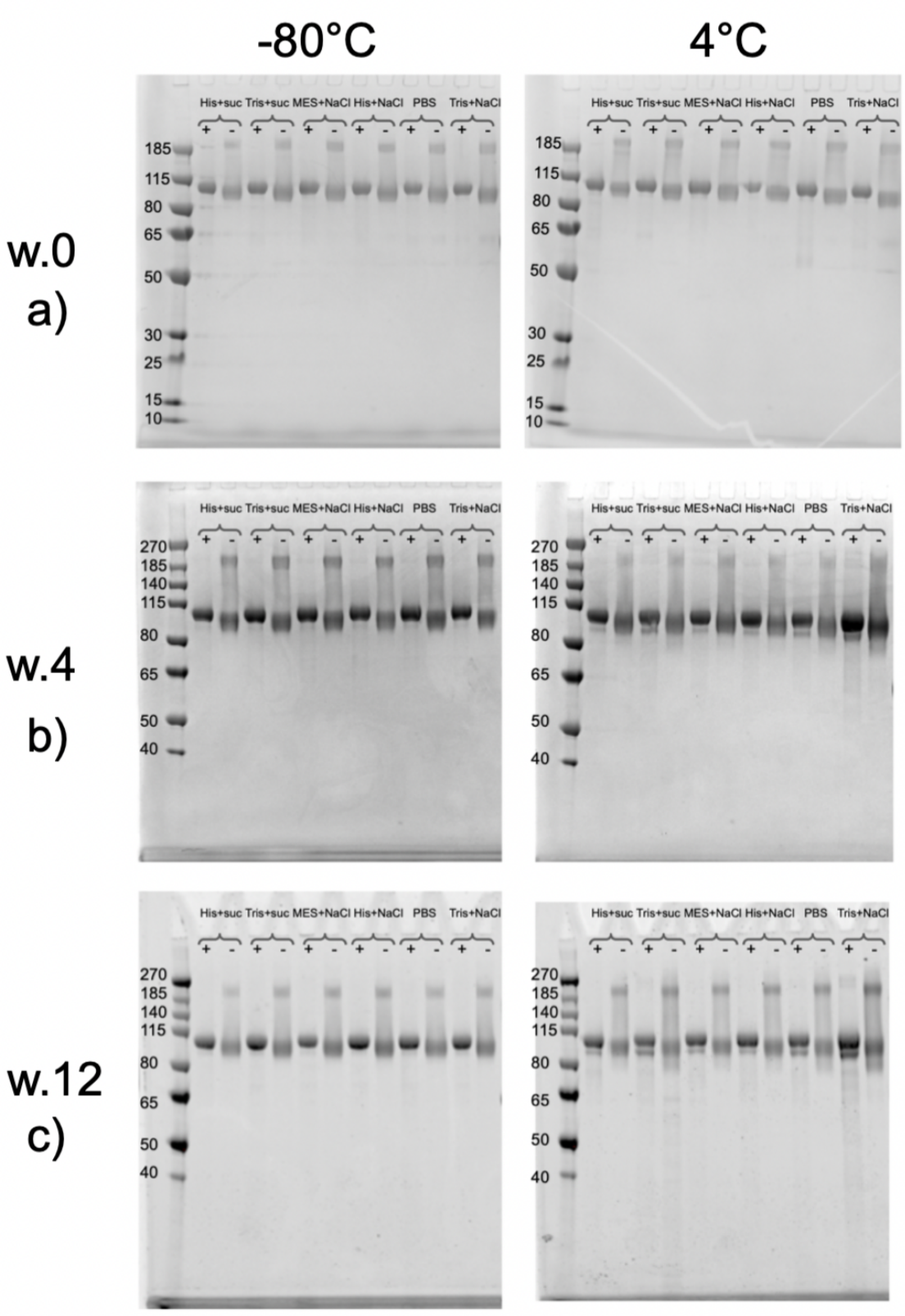

Figure 30a, 30b & 30c. SDS-PAGE gels from weeks 0, 4 and 12, stored in 4°C & -80°C respectively. Interpretation of legends; His = Histidine, suc = sucrose, Tris = Tris-HCl, += With DTT (DTT+), -= Without DTT (DTT-). The unit of the protein ladder seen to the left in all figures is kDa.

In all gels seen in figures 30a, 30b and 30c above, a clear band is seen around 104kDa in the wells loaded with DTT dye (+) and around 100 kDa in the wells without DTT (-). In the 4°C samples, a new band appears just beneath the strongest band around 94kDa over the weeks. Furthermore, the bands are slightly more smeared in the 4°C gels from weeks 4 and 12.

Using ImageQuant, the percentages of each band in a well could also be calculated. In figure 31 below, the average percentage of the strongest band at 104kDa is compared between the buffers with sucrose and the buffers with NaCl. In addition, means calculated from samples stored in 4°C are marked in yellow whereas the means calculated from samples stored in -80°C are marked in red. The error bars seen in the figure were created based on measurements from weeks 0 and week 1 of the buffers with each respective tonicity provider.

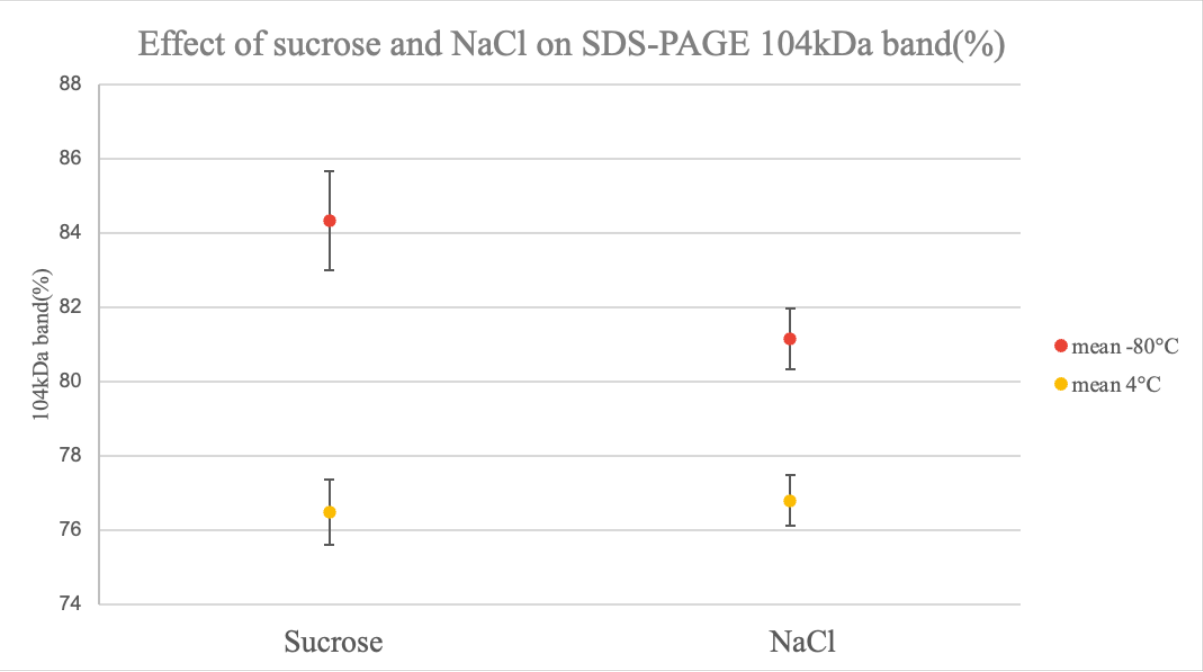

Figure 31. 104kDa band percentages in sucrose and NaCl buffers respectively, measured in ImageQuant analysis of the SDS-PAGE gels from weeks 0 and 1.

Generally, samples stored in -80°C have a higher band percentage. Furthermore, the sucrose buffers tend to have a higher band percentage in the samples stored in -80°C.

SE-HPLC

In figure 32a and 32b below, chromatograms obtained during week 2 from samples loaded with histidine NaCl buffer stored in -80°C and 4°C respectively, are seen. These results are representative for all the buffers over all five weeks. In appendix 4.2, chromatograms from all five weeks can be found of the different buffers stored in -80°C and 4°C.

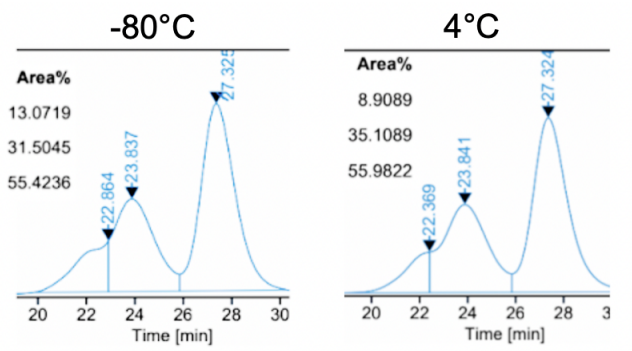

Figure 32a & 32b. SE-HPLC Chromatograms from week 2 of the rVAR2-aCD3 protein in histidine NaCl buffer stored in -80°C and 4°C.

No major differences could be observed by the naked eye between the chromatograms from the SE-HPLC of the different buffers from week to week. In appendix 4.2, it can be seen that the peak observed around 22 min, sometimes seemed to appear and disappear between the weeks.

SEC-MALS

The results from SEC-MALS performed on the original protein sample during week 2 of the tonicity study are seen in figure 33 below.

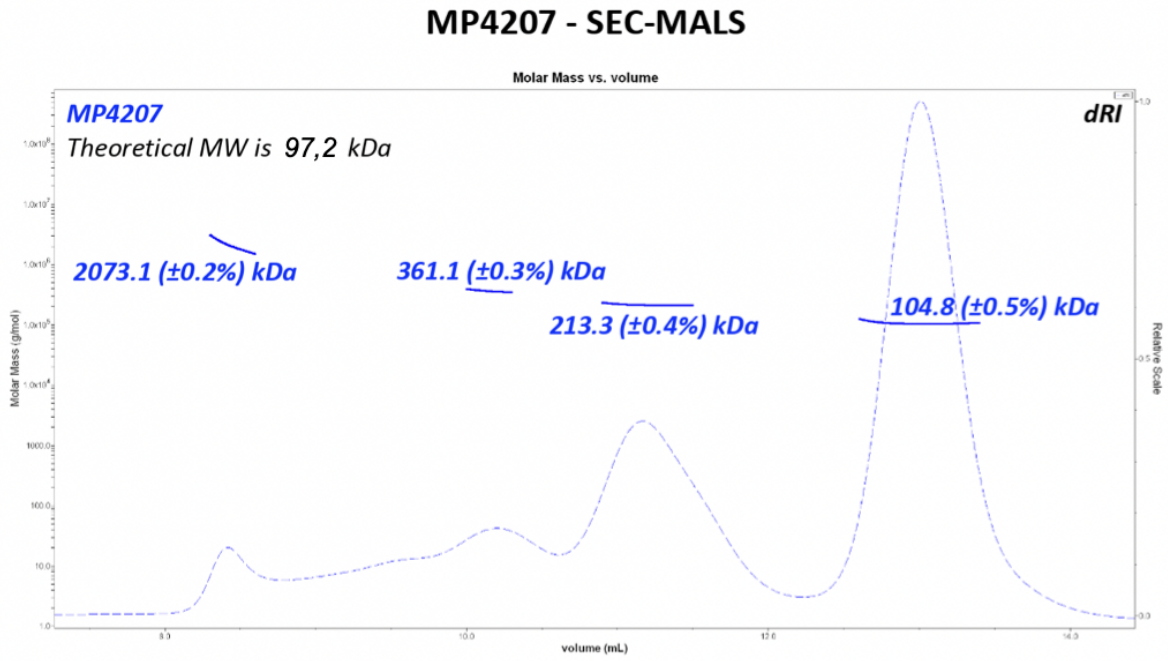

Figure 33. Chromatogram retrieved from SEC-MALS analysis of the original protein sample in PBS buffer.

In the top left corner of the figure, the theoretical molecular weight of the protein of 97.2 kDa is seen. The smallest peak identified by SEC-MALS had a size of 104.8 kDa. Furthermore, two larger molar masses were identified in the sample at 213.3 kDa and 361.1kDa respectively, and also a larger mass of 2073.1 kDa. In addition, it is seen that the three peaks of the smaller molar masses have a homogenous size distribution within each peak, indicated by the horizontal lines near the molar masses in the figure.

In figure 34 below, a zoomed in figure of the two smaller peaks is presented. The blue text indicates the full molar mass that could be identified for each peak. From the refractive index it was determined that a smaller part of the full molar mass was a sugar structure and not a protein. The green text in the figure represents the size of the smaller sugar structure that is attached to the larger protein structure, marked in red color.

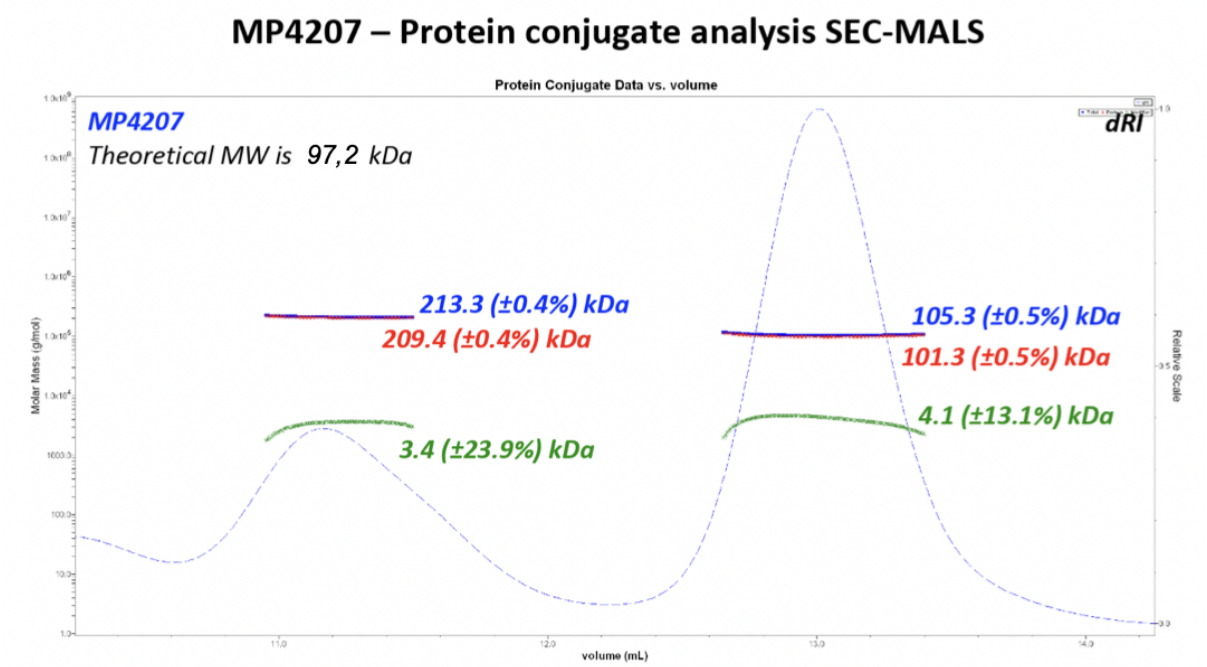

Figure 34. Zoomed in chromatogram retrieved from SEC-MALS analysis of the original protein sample in PBS buffer.

CSA ELISA

The results from CSA ELISA from weeks 0, 4, and 12 stored in both 4°C and -80°C and coated with decorin and HSPG respectively, are seen in figures 35a, 35b and 35c below.

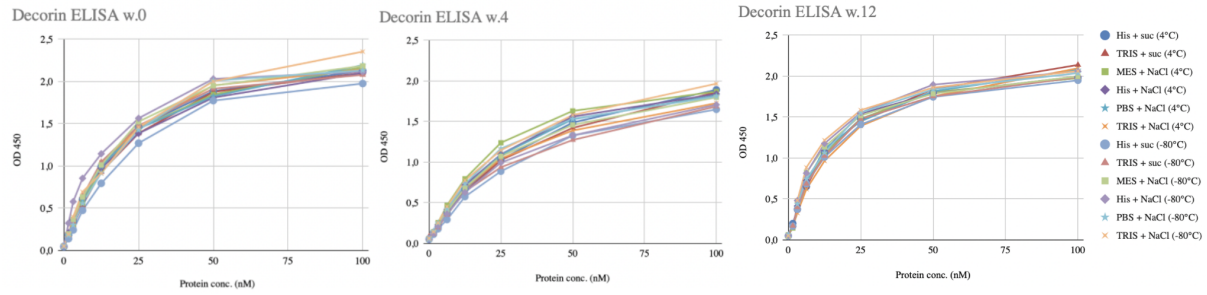

Figure 35a, 35b & 35c. Results from CSA ELISA, decorin binding performed during weeks 0, 4 and 12, in 6 different buffers stored in 4 °C and -80°C respectively.

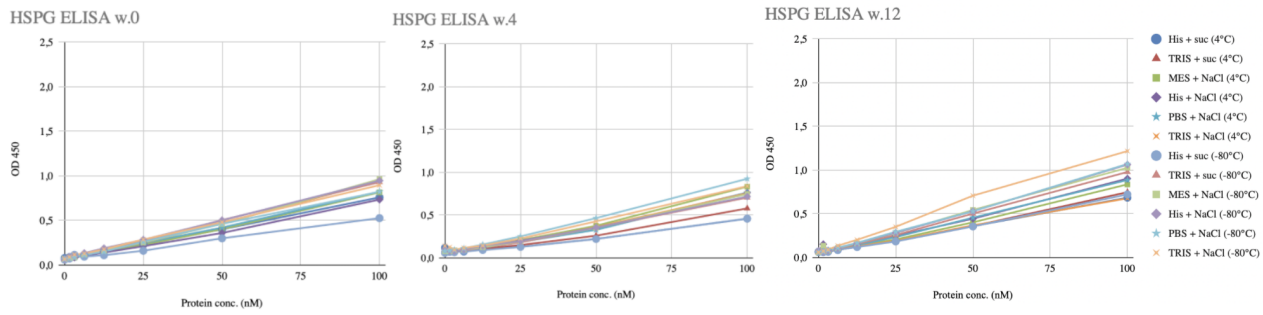

Figure 36a, 36b & 36c. Results from CSA ELISA, HSPG binding performed during weeks 0, 4 and 12, in 6 different buffers stored in 4 °C and -80°C respectively.

Overall, the binding is similar over the weeks. However, the decorin binding seems to decrease a bit over time and the HSPG spreads out more and more over the weeks. In figure 36 above it is seen that the HSPG binding w.12 (figure 36c) is slightly higher in the sample with tris-HCl NaCl stored in 4°C compared to the other buffers.

CD3 ELISA

The results from CD3 ELISA from weeks 1, 4 and 12 stored in both 4°C and -80°C, are presented in figure 37 below. The purple line is the binding of solely VAR2 (background signal) and the pink line is solely aCD3 (positive control). The fusion protein in the different buffers and VAR2 alone were detected by a V5 antibody, whereas the positive control was detected by a P260 IgG. As control, the fusion protein in PBS buffer was also detected by the P260 IgG, which is represented by the turquoise line.

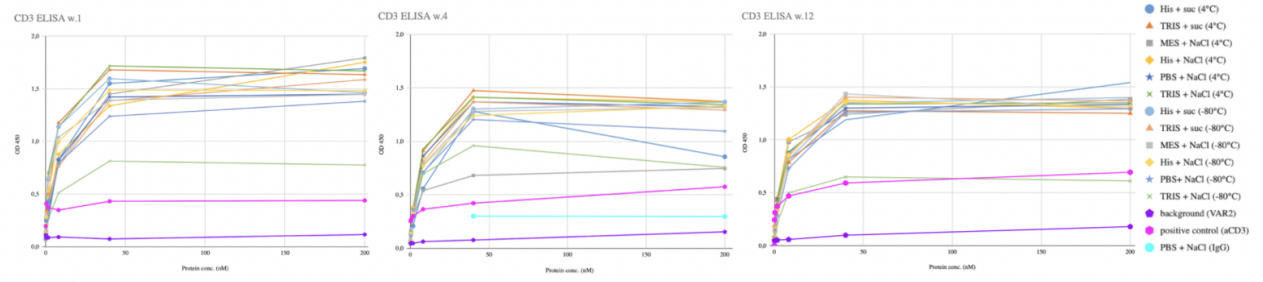

Figure 37a, 37b & 37c. Results from CD3 ELISA performed during weeks 1, 4 and 12, in 6 different buffers stored in 4 °C and -80°C respectively.

Overall, the binding fluctuates slightly over the weeks, but keeps a similar pattern. In all measurements the tris-HCl NaCl buffer stored in -80°C (light green curve with crosses) has a lower binding than the other buffers.

FACS

In figure 38 below, FACS results from weeks 2, 4 and 12 of the tonicity study, stored in both 4°C and -80°C can be seen. All measurements were performed on PBMCs from the same donor. In the results from week 1, the PBMCs were freshly used and not frozen before usage, in comparison to the results from the other measurements. The background binding arising from VAR2 alone is represented by the black line. The

protein concentrations and dilution series on the plate were changed over the weeks in order to find the linear range of the binding.

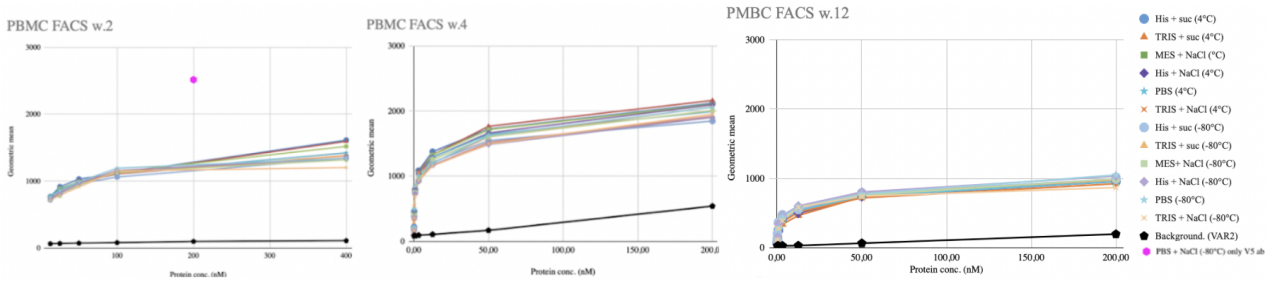

Figure 38a, 38b & 38c. Results from PBMC FACS during weeks 0, 4 and 12, in 6 different buffers stored in 4 °C and -80°C respectively.

The binding is similar between the buffers, however the geometric mean fluctuates between each measurement. The lowest geometric mean is observed in the week 12 measurement. The two buffers with lowest binding the week 12 measurement is tris-HCl stored in both 4°C and -80°C respectively, seen in figure 38c above and appendix 4.5.12.

DLS

The results from DLS performed during week 4 of the tonicity study on the protein in PBS buffer is seen in figures 39, 40 and 41 below. Figure 39 represents the protein stored in -80°C being measured at 22°C. The two figures below 40 and 41 represent the protein after 5 minutes of heat shock at 40°C and 55°C respectively, and then measured at 22°C.

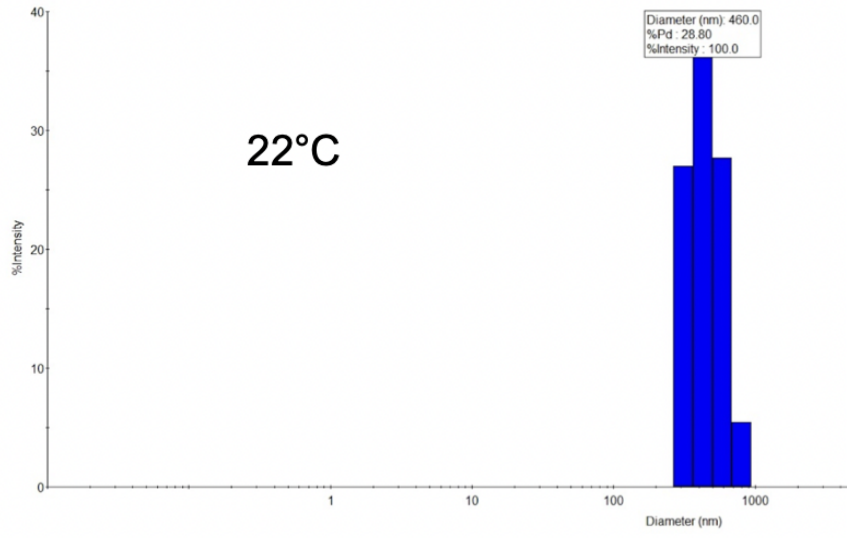

Figure 39. DLS results performed in week 4 on the original protein sample.

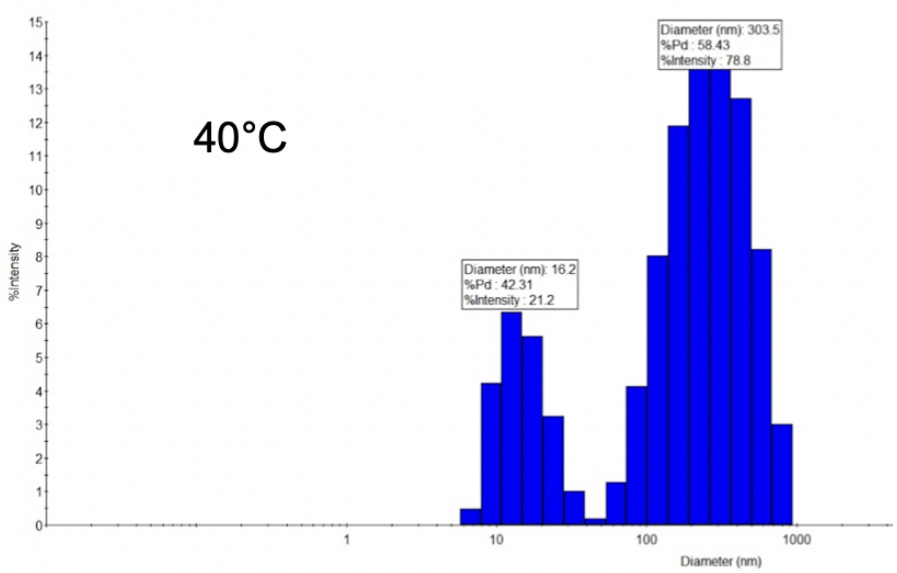

Figure 40. DLS results performed in week 4 on the original protein sample after 5 minutes of heat shock at 40°C.

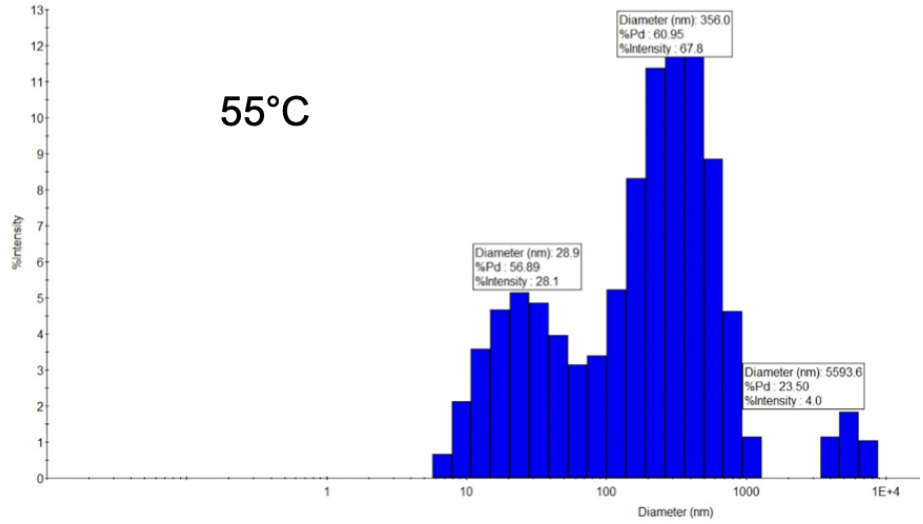

Figure 41. DLS results performed in week 4 on the original protein sample after 5 minutes of heat shock at 55°C.

A broader size distribution is observed in the sample after heat shock. The sample heat shocked at 55°C is even more distributed than the sample shocked at 40°C.

SAS JMP

In figure 42 below, the prediction profile of an optimal storing temperature and pH according to the analytical software SAS JMP is presented. The inputs were: maximized peak% at 27 minutes from SE-HPLC, maximized band% at 104kDa from SDS-PAGE (DTT+) and minimized Kd values from CSA ELISA with decorin. The outputs were storing temperature (4°C or -80°C) and pH (6-8).

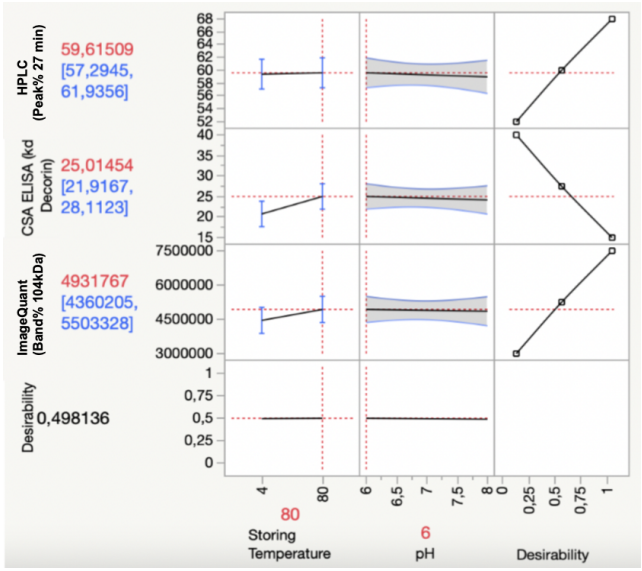

Figure 42. Optimal pH and storing temperature predicted by SAS JMP.

SAS JMP suggests a storing temperature of -80°C and a pH of 6.

6.4 Stress study

In the following section the results from three physical stress tests performed over 5 weeks are presented. The results from the pre-study are found in appendices 5.1.1 and 5.2.2.

NanoDSF

The NanoDSF measurement showed similar results as seen in the previous initial study and tonicity study with buffers with pH <7 having two peaks and buffers with pH >7 having one peak in the first derivative. These results are found in see appendix 5.4.

SDS-PAGE: Time point 0

The results obtained from SDS-PAGE in week 0 of the stress study can be seen in figure 43 below. In the following results from all three stress tests, this gel is considered as the starting point (TP0, time point 0).

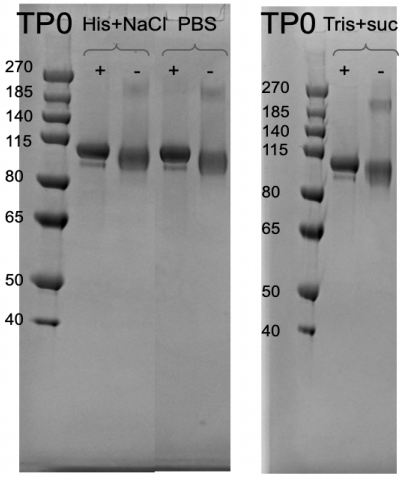

Figure 43. SDS-PAGE gel from the starting point of the stress studies (time point 0=TP0).

Similar patterns are observed for all three buffers. In the wells loaded with DTT dye (+), a strong band around 104kDa can be seen, as well as another thinner band just beneath at 94kDa. In the wells without DTT dye (-) a stronger band around 100 kDa is observed and a thinner band around 200 kDa can be seen.

SDS-PAGE: Stress test 1

The results obtained from the SDS-PAGE measurement of stress test 1, measured after 19 days (time point 19 = TP19) in room temperature, are seen in figure 44 below. As nothing was left of the PBS sample at this time point, the PBS sample used in the pre-study was loaded on the gel instead, which then had been stored at room temperature for 38 days (time point 38 = TP38). Results from SDS-PAGE measured at time points 3, 6 and 11 days can be seen in appendix 5.1.2.

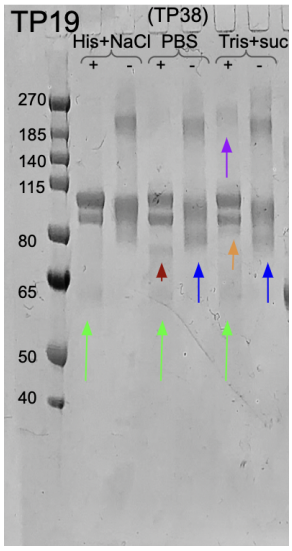

Figure 44. SDS-PAGE gel from the end of stress test 1 (room temperature). Histidine buffer with NaCl and tris-HCl buffer with sucrose measured at time point 19, and PBS sample measured at time point 38. Colored arrows indicate new bands appearing on the gel. The same color is used when the same band appears in more than one buffer.

In all three buffer samples, a new band around 60 kDa had appeared in the wells with DTT dye (+), marked out with green arrows. Furthermore, in all wells loaded without DTT dye (-) for all three buffers, an additional band is seen around 300kDa. In addition, the strongest band at 104kDa observed in the wells with DTT dye (+) has become thinner and the band beneath at 94kDa seems to have become thicker in all buffers in comparison to the starting point. In the well loaded with the tris-HCl buffer sample with sucrose and DTT dye (+) yet another new band has appeared underneath that band at 80kDa, which is marked out with a yellow arrow. One more new band was observed in this well of around 208kDa, marked with a purple arrow. This band was first observed after 3 days in the tris-HCl buffer, see appendix 5.1.3.

Furthermore, in the well loaded with PBS sample and DTT dye (+) another new band had appeared around 70kDa, marked with a red arrow, which also was seen during previous pre-study measurements after 7 days in room temperature (see appendix 5.1.1). In the two wells loaded with PBS buffer and tris-HCl sucrose

buffer samples without DTT dye (-), two new bands also appeared around 75kDa, marked out with dark blue arrows. This band was first observed after 11 days in tris-HCl sucrose buffer and after 10 days in PBS buffer (appendices 5.1.1 and 5.1.2).

An overview of the band percentages obtained from an ImageQuant analysis from wells loaded with DTT dye (+), are found in figures 45 and 46 below. Bands marked with colored arrows in figure 44 are marked out with a matching color in the graph below.

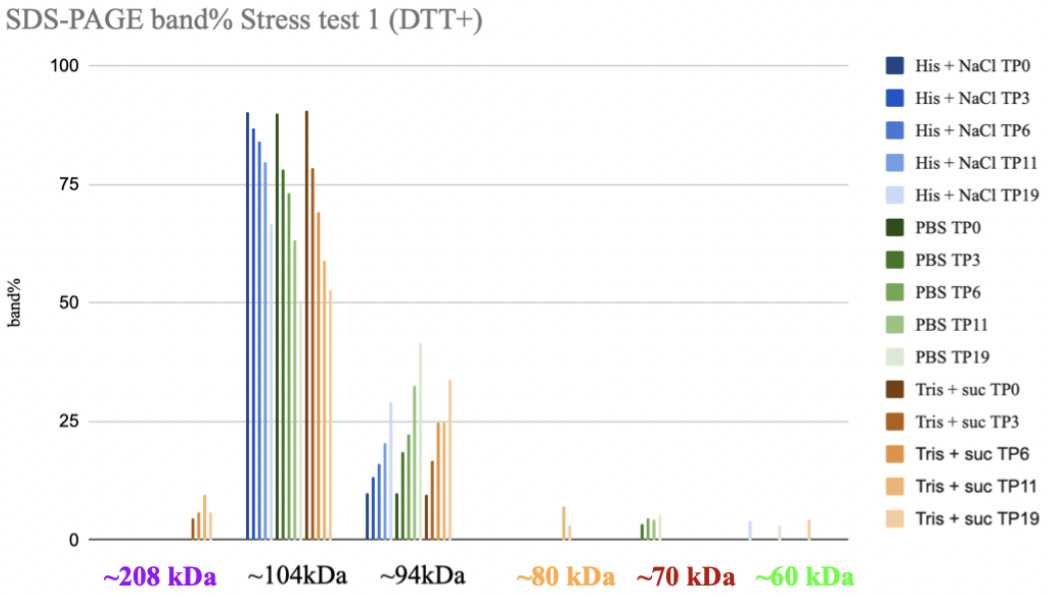

Figure 45. Changes in band percentages observed over time obtained from image analysis of the SDS-PAGE gels using ImageQuant. The data was obtained from stress test 1 (room temperature) from the wells loaded with reducing agent DTT (+). The colors on the x-axis refer to the colored arrows on the gel in figure 44.

Figure 46 below zooms in on the decrease of the 104kDa band in the different buffers over the measured time points.

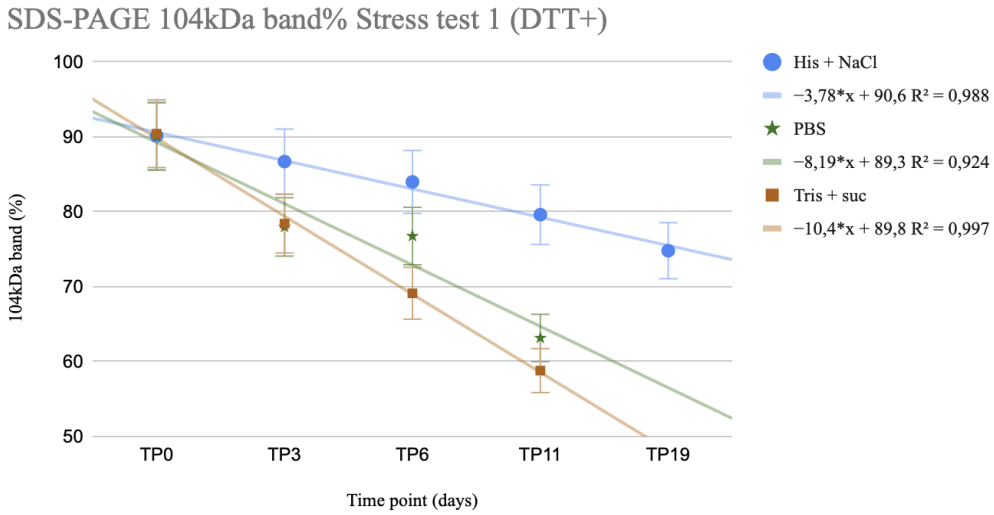

Figure 46. Zoomed in decrease of the 104kDa band percentage in the histidine NaCl, PBS and tris-HCl sucrose buffers.

As seen in both figure 45 and 46 above, the largest decrease of the 104 kDa band is seen in the tris-HCl sucrose buffer and the smallest decrease is seen in the histidine NaCl buffer.

SDS-PAGE: Stress test 2

The results obtained from the SDS-PAGE measurement of stress test 2, measured after 19 days (time point 19) in room temperature with 30 minutes rotation each day, are seen in figure 47 below. Results from SDS-PAGE measured at time points 3, 6 and 11 can be seen in appendix 5.1.3.

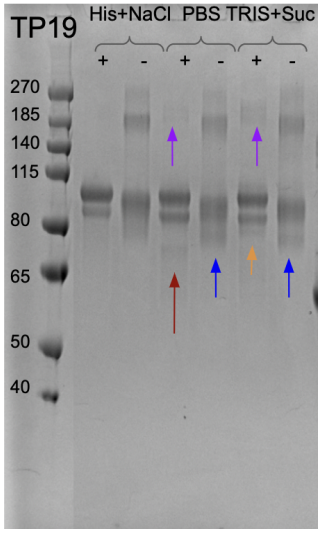

Figure 47. SDS-PAGE gel from the end of stress test 2 (room temperature and rotation). All samples were measured at time point 19. Colored arrows indicate new bands appearing on the gel. The same color is used when the same band appears in more than one buffer.

In the wells loaded without DTT dye (-) for all the buffers, an additional band is observed around 300kDa. In addition, the strongest band observed (104kDa) in the wells with DTT dye (+) has become thinner and the band at 94kDa seems to have become thicker in all the buffers in comparison to the starting point. In the well loaded with the tris-HCl sucrose buffer sample with DTT dye (+) yet another new band has appeared underneath that band at 80kDa, which is marked out with a yellow arrow. In this well and in the well loaded with PBS buffer, also with DTT dye (+), another new band is observed around 208kDa, marked with purple arrows. This band was first observed after 3 days in the tris-HCl buffer, see appendix 5.1.3.

In the PBS sample with DTT dye (+) another new band had appeared around 70kDa, marked with a red arrow, which was first observed after 3 days (see appendix 5.1.3). Furthermore, in the two wells loaded with PBS buffer and tris-HCl sucrose buffer samples without DTT dye (-), two new bands also appeared around 75kDa, marked out with dark blue arrows. These were first observed after 3 days in both buffers, seen in appendix 5.1.3.

An overview of the band percentages obtained from an ImageQuant analysis from wells loaded with DTT dye (+), are found in figures 48 and 49 below. Bands marked with colored arrows in figure 47 are marked out with a matching color in the graph below.

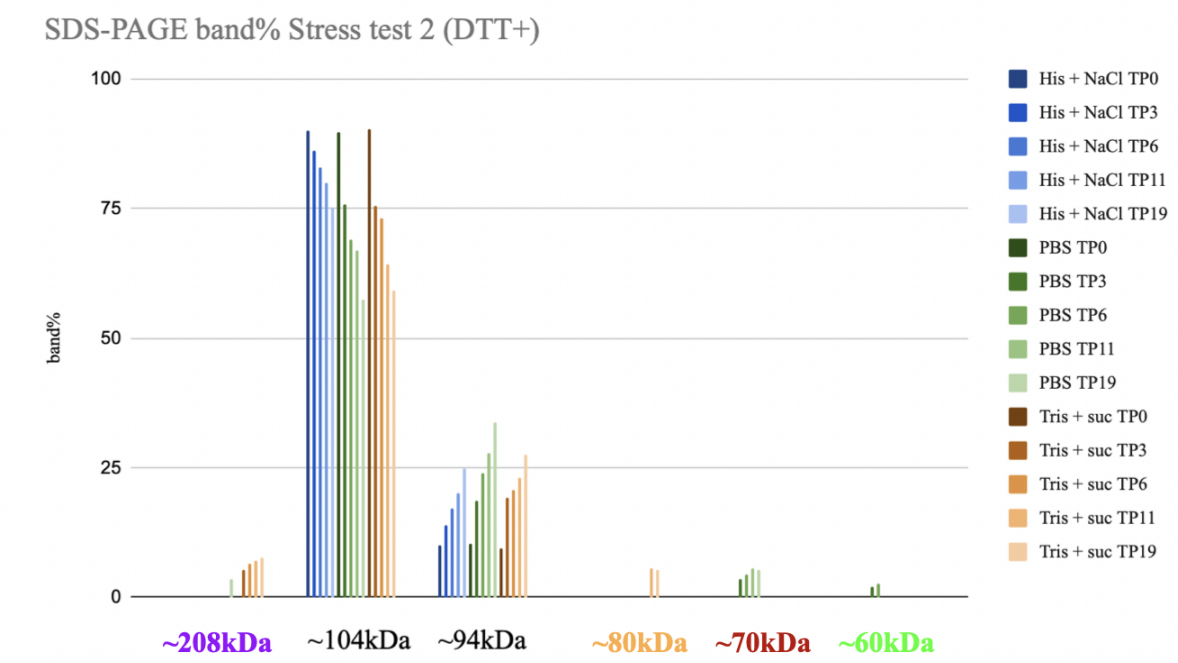

Figure 48. Changes in band percentages observed over time obtained from image analysis of the SDS-PAGE gels using ImageQuant. The data was obtained from stress test 2 (room temperature + rotation) from the wells loaded with reducing agent DTT (+). The colors on the x-axis refer to the colored arrows on the gel in figure 47.

Figure 49 below zooms in on the decrease of the 104kDa band in the different buffers over the measured time points.

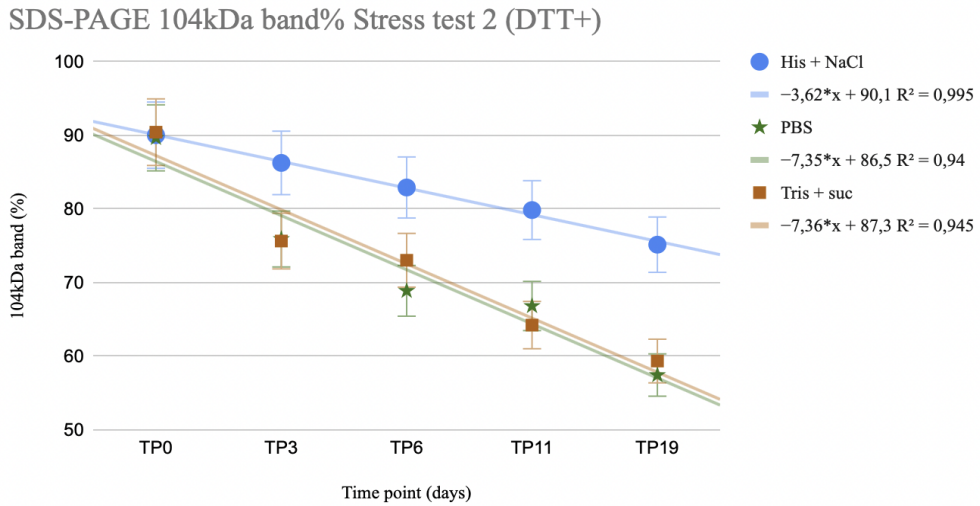

Figure 49. Zoomed in decrease of the 104kDa band percentage in histidine NaCl, PBS and tris-HCl sucrose buffer.

As seen in both figure 48 and 49 above, the smallest decrease of the 104 kDa band is seen in the histidine NaCl buffer. PBS and tris-HCl sucrose samples have a similar higher decrease.

SDS-PAGE: Stress test 3

The results obtained from an SDS-PAGE measurement of stress test 3, measured after 6 cycles of freezing and thawing (abbreviated FT6), are seen in figure 50 below. Results from SDS-PAGE at FT3 can be seen in appendix 5.1.4.

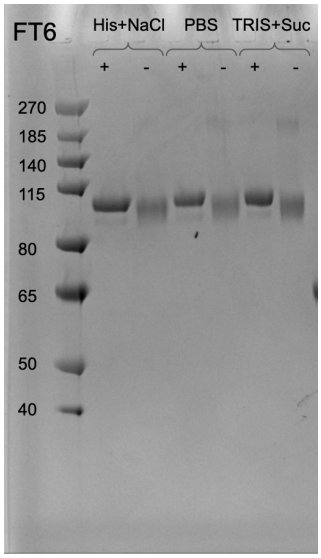

Figure 50. SDS-PAGE gel from the end of stress test 3 (freezing and thawing). All samples were measured after 6 cycles of freezing and thawing.

No changes or new bands were observed in comparison to the starting point (time point 0, seen in figure 43).

MS

From an SDS-PAGE gel (Pre-study TP7, appendix 5.1.1), the strong band around 104kDa as well as the band right beneath of 94kDa and a new appearing band at 70kDa (red arrow in figures 44 and 47) were cut out and sent for further analysis by mass spectrometry. 21.6% of the 104kDa band and 10.9% of the 94kDa band could be detected. 0% of the band at 70 kDa could be detected. These results are found in appendix 9.

SE-HPLC: Time point 0

The results obtained from SE-HPLC in week 0 of the stress study can be seen in figures 51a, 51b and 51c below. In the following results from all three stress tests, these chromatograms are considered as the starting points (time point 0).

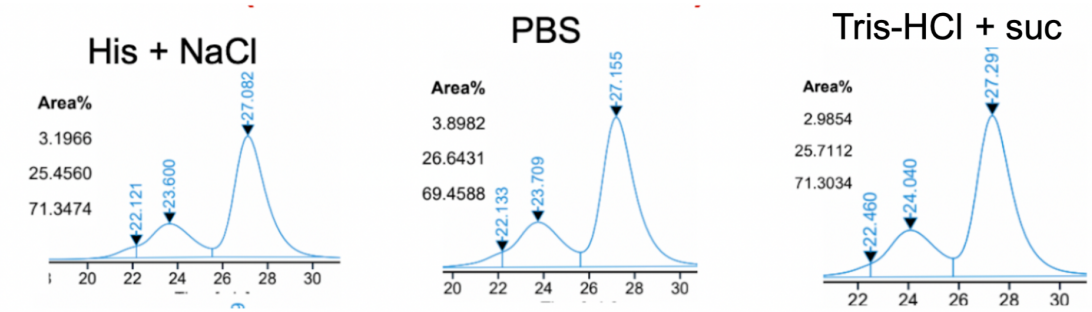

Figure 51a, 51b & 51c. Chromatograms obtained from an SE-HPLC at the starting point of the stress studies (time point 0=TP0).

Similar patterns were observed for all three buffers. Three peaks are observed at around 27 minutes, 24 minutes and 22.5 minutes, respectively, where the peak at 27 minutes has the highest intensity.

SE-HPLC: Stress test 1

The results obtained from the SE-HPLC measurement of stress test 1, measured after 11 days (time point 11 = TP11) in room temperature, are seen in figures 52a, 52ba and 52c below.

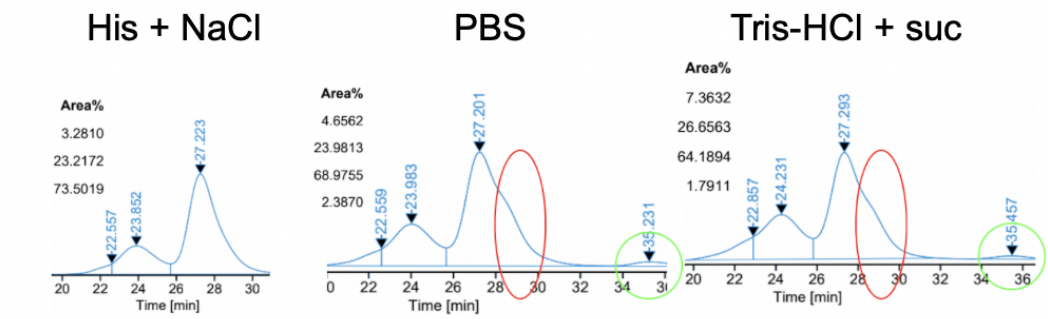

Figure 52a, 52b & 52c. Chromatograms obtained from SE-HPLC measurement of stress test 1 (room temperature) measured at time point 11 (TP11).

In addition to the three peaks at 27 minutes, 24 minutes and 22.5 minutes respectively, observed from the start (figure 51), two new peaks started to show up in the PBS buffer and tris-HCl sucrose buffer samples. One of the peaks was seen around a retention time of 29 minutes (marked in red) and the other one at around 35 minutes (marked in green). No new peaks were observed in the histidine buffer with NaCl. In the measurement at time point 19 the same pattern was seen again, see appendix 5.2.3.

In appendix 5.2.3, changes in peak percentages over time obtained from SE-HPLC chromatograms can be observed. The analyzed chromatograms were measured at time points 0, 3, 6, 11 and 19 respectively.

SE-HPLC: Stress test 2

The results obtained from the SE-HPLC measurement of stress test 2, measured after 11 days (time point 11 = TP11) in room temperature, are seen in figures 53a, 53b and 53c below.

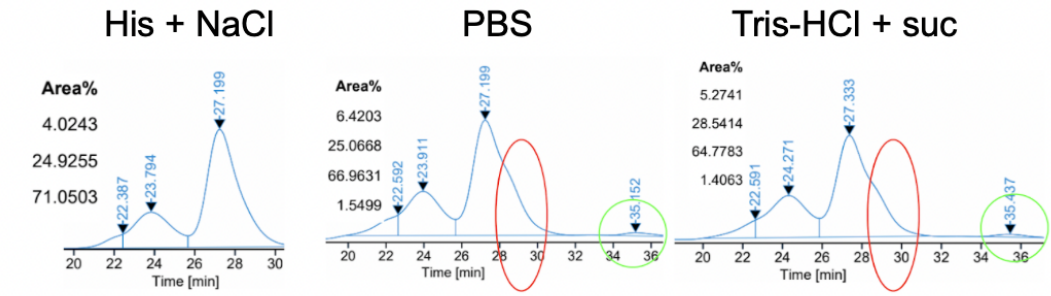

Figure 53a, 53b & 53c. Chromatograms obtained from SE-HPLC measurement of stress test 2 (room temperature and rotation) measured at time point 11 (TP11).

Similar to the results seen in stress test 1, two new peaks started to show up in the PBS buffer and tris-HCl sucrose buffer samples at 29 minutes (marked in red) and 35 minutes (marked in green). No new peaks were observed in the histidine buffer with NaCl. In the measurement at time point 19 the same pattern was seen again, see appendix 5.2.4.

In appendix 5.2.4, changes in peak percentages over time obtained from SE-HPLC chromatograms can be observed. The analyzed chromatograms were measured at time points 0, 3, 6, 11 and 19 respectively.

SE-HPLC: Stress test 3

The results obtained from the SE-HPLC measurement of stress test 3, measured after 6 cycles of freezing and thawing (abbreviated FT6), are seen in figure 54a, 54b and 54c below.

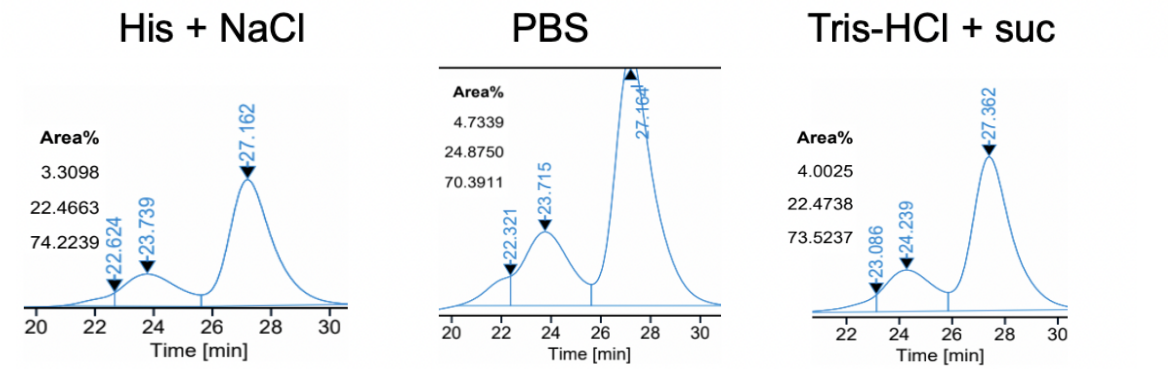

Figure 54a, 54b & 54c. Chromatograms obtained from SE-HPLC measurement at the end of stress test 3 (freezing and thawing). All samples were measured after 6 cycles of freezing and thawing.

The same three peaks seen from the start (figure 51) were observed after 6 cycles of freezing and thawing. Nothing new appeared in the chromatograms. However, the peak intensity was increased in the PBS buffer as seen in figure 54 above.

NanoDrop

Each time before running the other analytical methods, protein concentration was measured by NanoDrop. It was observed that the protein concentration seemed to increase in the sample stored in the PBS buffer over time. The increase in PBS buffer samples was also observed in the pre-study and in stress tests 1 and 2. The measured concentration at the starting point was 0,809 mg/mL and at the ending point of stress 3 after 6 cycles of freezing and thawing the concentration was measured to 1,34mg/mL. The end concentrations of the other studies are seen in appendix 6.2.

CSA ELISA: Time point 0

The results obtained from CSA ELISA in week 0 of the stress study can be seen in figure 55a and 55b below. In the following results from all three stress tests, these figures are considered as the starting points (time point 0).

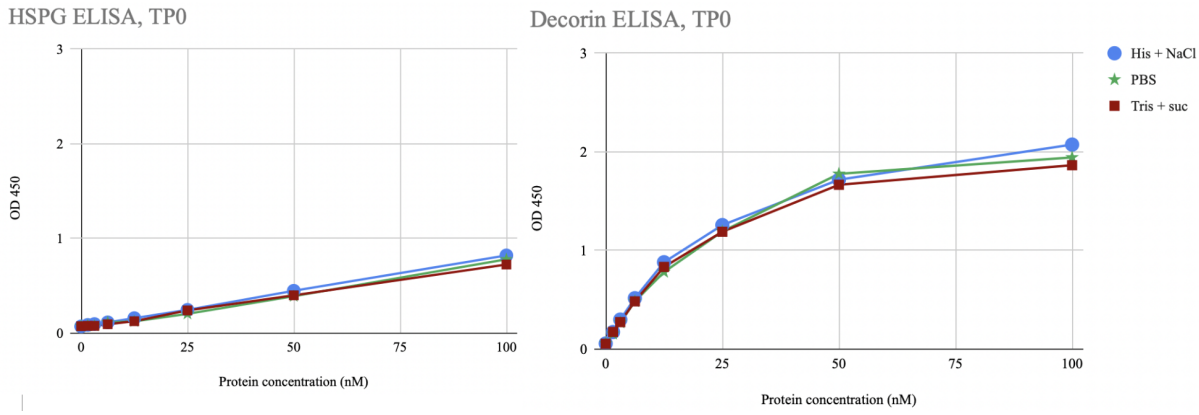

Figure 55a & 55b. CSA ELISA results at the starting point of the stress studies (time point 0=TP0).

All buffers have very similar binding to both decorin and HSPG.

CSA ELISA: Stress test 1

The results obtained from the CSA ELISA measurement of stress test 1, measured after 11 days (time point 11 = TP11) in room temperature, are seen in figure 56 below.

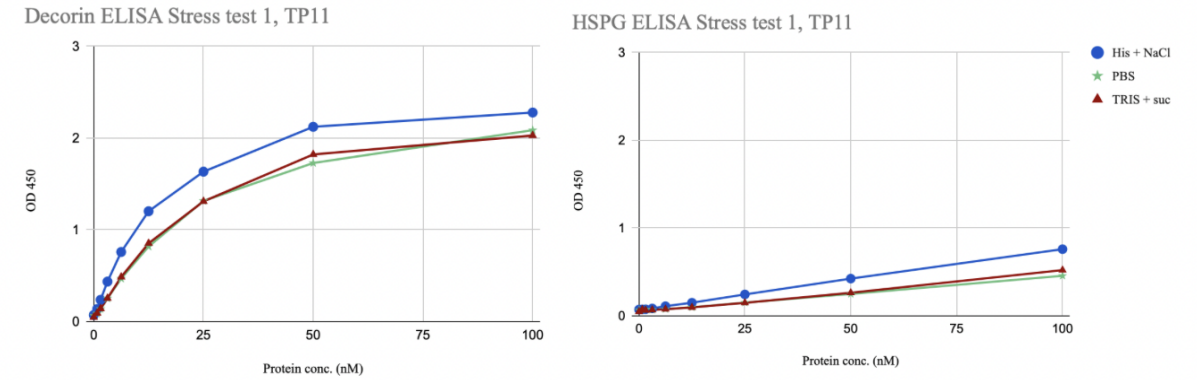

Figure 56a & 56b. Results from CSA ELISA of stress test 1 (room temperature) measured at time point 11 (TP11).

A higher binding both towards decorin and HSPG is seen in the sample with histidine buffer with NaCl in comparison to the other buffers. The samples with tris-HCl sucrose and PBS buffers show similar binding. The measurement at the time point 19 shows similar results as seen in figure 56a and 56b above (see appendix 5.3.1).

CSA ELISA: Stress test 2

The results obtained from the CSA ELISA measurement of stress test 2, measured after 11 days (time point 11 = TP11) in room temperature, are seen in figure 57a and 57b below.

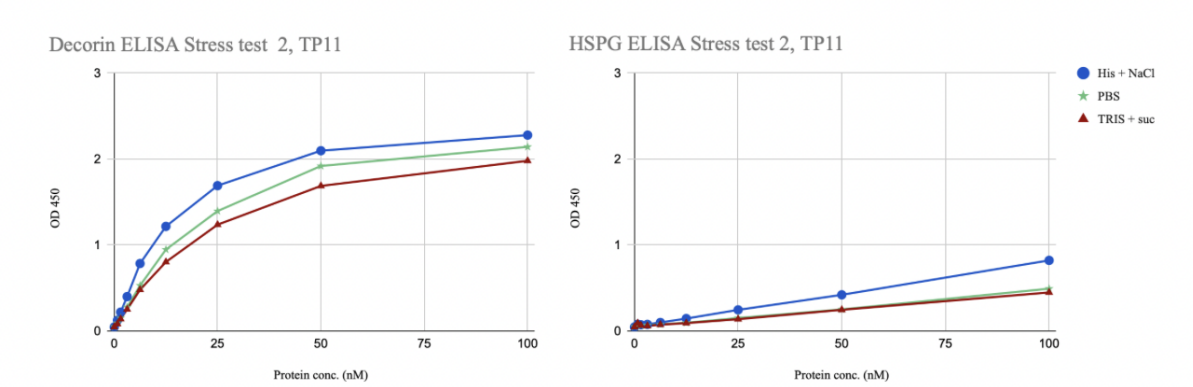

Figure 57a & 57b. Results from CSA ELISA of stress test 2 (room temperature and rotation) measured at time point 11 (TP11).

A higher binding both towards decorin and HSPG is seen in the sample with histidine buffer with NaCl in comparison to the other buffers. The PBS sample seems to have a higher binding to decorin than the tris-HCl sucrose sample, but they have similar binding to HSPG. The measurement at the time point 19 shows similar results as seen in figure 57 below (see appendix 5.3.2).

CSA ELISA: Stress test 3

The results obtained from the CSA ELISA measurement of stress test 3, measured after 6 cycles of freezing and thawing (abbreviated FT6), are seen in figure 58a and 58b below.

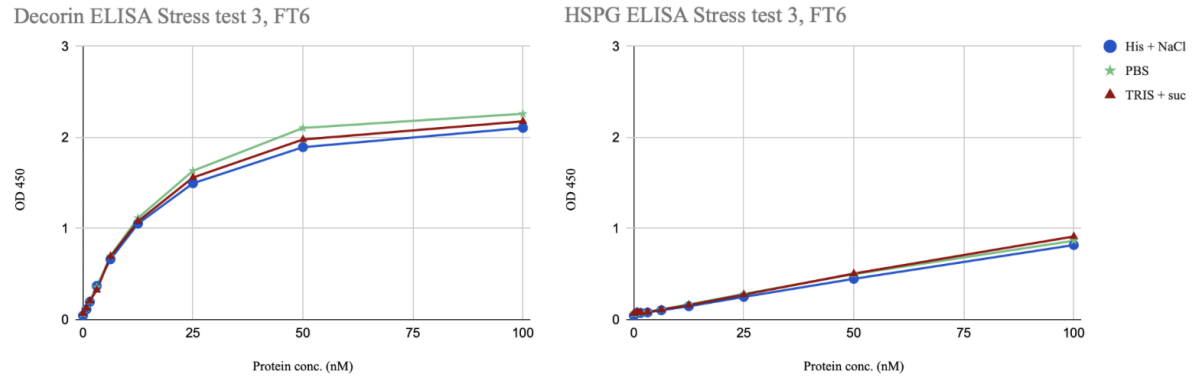

Figure 58a & 58b. Results from CSA ELISA at the end of stress test 3 (freezing and thawing). All samples were measured after 6 cycles of freezing and thawing.

All buffers bind similarly to both decorin and HSPG.

NGC

Due to low concentrations of the protein samples, only very small volumes with very low concentrations of the monomers and dimers respectively could be fractionated using NGC. Results from this assay as well as from the SDS-PAGE, SE-HPLC and ELISA measurements performed on the fractionated proteins are found in appendix 10.

7. Discussion

The following sections will contain discussions of the results that have been presented in the previous section.

7.1 *In silico* modelling

In figure 23 a simulated three-dimensional structure of the rVAR2-aCD3 fusion protein is presented. This image can be viewed as a suggestion to how the folded complex would look, however it is important to know that the real structure is still unknown. As the exact binding site in the VAR2-part of the complex has yet not been identified, it is quite difficult to predict its folding. To identify real protein structures, analytical techniques such as X-ray crystallography, NMR spectroscopy or electron microscopy could be used. (Protein data bank, 2021)

In the amino acid maps found in appendices 1.1 and 1.2 it was found that there were a few sites in the scFv potentially prone to degradation. The most common risk of degradation was through deamidation of asparagine and glutamine amino acids within the CDR-regions. Risks of oxidation and light-induced oxidation were also found. To prevent these effects, the formulation could be further optimized. Deamidation usually occurs in neutral or alkaline environments (Wang, W.,1999). To prevent deamidation, formulations of lower pH are commonly used. In addition, antioxidants can be added to prevent oxidation and the pharmaceutical could be kept in a non-transparent container to avoid light-induced oxidation.

7.2 Initial study

In the following section, the results from the initial study are discussed.

NanoDSF

In figure 24, it is seen that the protein in the citrate buffer (pH 3.3) behaves quite differently than the other samples. In the top graph of the figure, it is shown that the fused protein unfolds at a much lower temperature, 37.5 °C, in comparison to the other buffers with a melting temperature ranging between 68.7 °C - 70.8 °C. The buffer with the second lowest melting temperature is the acetate buffer (pH 4.6). In a similar stability study on an IgG antibody in different buffer formulations performed by Chavez B. K. et al., acetate buffer was eliminated due to formation of visual precipitation (Chavez, B. K. et al., 2015). Precipitation happens when the proteins denature, aggregate and fall out of the solution (Stone, J., 2017).

In the first derivatives (bottom graph in figure 24) of the acetate buffer (pH 4.6), histidine buffer (pH 6) and the MES buffer (pH 6), two peaks are observed. In previous NanoDSF measurements it was found that the VAR2 protein alone produced in E. coli has a T_m around 70°C. Hence, the second peak appearing around 70°C could be interpreted to correspond to the VAR2-part of the protein and that the peak that is observed would then correspond to the scFv of the protein (aCD3).

Interestingly, only one peak is seen in the PBS buffer (pH 7.5) and in the tris-HCl buffer (pH 8.0) samples. This could indicate that the whole complex unfolds at the same time instead. As this is a pattern only seen in the buffers of higher pH, the behavior is thought to be pH dependent. It is difficult to say if one or two peaks

is preferred. However, as the one peak in the buffers of higher pH is seen at a lower temperature, one could interpret it as the high pH makes VAR2 less stable since it unfolds at an earlier temperature. Still, it should be noted that as high temperatures as 60-70°C are circumstances the protein complex probably never will be exposed during storage or administration.

SDS-PAGE

In the results seen in figure 25, a clear band is seen around 104kDa in the wells loaded with DTT dye (+) and around 100 kDa in the wells without DTT (-). These bands are thought to represent the monomer of the protein which has a theoretical size of 97kDa. The gel shift between 97 kDa and 104 kDa is further discussed in the 7.3 discussion of the tonicity study. In the samples loaded with dye without DTT (-), bands at around 200kDa and sometimes also 300kDa are also seen, which are thought to represent dimers and trimers, respectively.

Most of the samples show bands indicating proteins of smaller size when the loading dye without DTT (-) was added, and larger sizes when the loading dye with DTT (+) was added. This agrees with literature, as DTT has a reducing effect on the proteins helping them to preserve their original structure, while the dyes without DTT (-) have a non-reducing effect breaking the bonds of the secondary structure. (Thermofisher, 2020) However, the difference in protein size is less apparent in the wells loaded with citrate buffers (pH 3.3) compared to the other buffers, seen in both figures 25a and 25b. In the citrate buffer samples, both bands appear at the same smaller protein size, indicating that the bonds broken by the loading dye without DTT (-) seem to already be broken in the sample with DTT(+). This result could indicate that the citrate buffer is an unsuitable choice of buffer for the VAR2-aCD3 protein.

Another observation from the SDS-PAGE results is that the band from the tris-HCl buffer (pH 8) without DTT (-) is slightly thicker and more smeared compared to the other samples, which could be an indication of poor sample quality.

In both gels measured during week 2 (appendices 3.1.1 and 3.1.2), new bands had suddenly appeared on the gel in most of the samples around 65 kDa in wells loaded with DTT dye (+) and 55 kDa in wells without DTT (-). As these bands of 66.6 kDa were not seen during the previous measurements, they were thought to be contaminants, possibly from BSA (Merck, 2021). As the same samples were frozen and thawed and used over and over again in the initial study it is not very surprising that they eventually were contaminated.

SE-HPLC

In the chromatogram seen in figure 26 three peaks can be seen at around 22.5 min, 24 min and 27 min respectively. As the largest compounds have the shortest retention time in an SE-HPLC measurement, it is thought that the first peak appearing at 22.5 min represents a trimer of the fusion protein, the second peak at 24 min represents a dimer and the last peak at 27 min represents the monomer. This theory correlates well to the intensity of the peaks, as around 75% of the sample consists of the monomer, 23% consists of the dimer and only 2% of the trimer. However, as seen in figure 26, the dimer and trimer peaks are not very well separated, and the method could therefore be more optimized for further experiments in terms of choices of column or flow rate.

CSA ELISA

As decorin is an antigen found only on cancer cells, strong binding is desired. On the contrary, HSPG is an antigen found on all animal cells and therefore low binding is desired. (Christianson, H. C., & Belting, M., 2014). Overall, a clearly lower binding towards HSPG and higher binding towards decorin is seen in all samples (figures 27a and 27b), as desired. Furthermore, no major differences in binding were observed between the 4°C and -80°C samples.

It is seen that the sample with citrate buffer (pH 3.3) seems to bind the strongest to decorin, however it also binds HSPG the strongest which is undesired. Furthermore, the second strongest binding towards HSPG is seen in the tris-HCl samples (pH 8).

7.3 Tonicity study

In the following section, the results from the tonicity study are discussed.

During the desalting of the protein into the histidine sucrose buffer, less amount of protein was obtained than desired. In literature, problems have been faced previously with the combination of histidine buffer and sucrose as tonicity provider. In an article from Baek, Y et al. (2017) it is stated that sucrose in histidine buffers can increase the hydrodynamic radius of monoclonal antibodies (Baek, Y. et al., 2017). If a similar mechanism occurred in the protein complex (containing a part of an antibody), an increased radius could affect the desalting process by entrapping the protein in the filter, hindering it from flowing through the column as intended.

NanoDSF

In the melting curves seen in figure 28, two different melting patterns were identified, either with one single peak or with two peaks. As presented in table 8, buffers with a pH >7 tended to have one peak and buffers with pH <7 had two peaks. These results were similar to what was seen in the initial study, confirming that a higher pH gives rise to a melting curve pattern with one peak. It is still difficult to decide which one of the two patterns that should be preferred, but the hypothesis of two peaks being preferred that was presented in the discussion of the initial study remains.

Due to the clear difference in melting curve patterns, it was decided to continue with buffers of both types (one peak and two peaks) for the upcoming stress study to see how this property could affect physical stability.

SDS-PAGE

The same reasoning as presented in the initial study discussion remains, with the band seen at 104 kDa in the wells with DTT dye (+) and 100 kDa in the wells without DTT (-) corresponding to the monomers. Furthermore, the bands at 200kDa in the wells loaded without DTT (-) thought to be the dimers in the initial study were also observed in the tonicity study, but no trimers (300kDa) were seen.

Using ImageQuant, the molecular weight of the protein thought to correspond to the monomer, was calculated to be around 104 kDa, see figure 29. As the theoretical molecular weight is lower than this (97.2 kDa) these results could indicate that the fused protein has been glycosylated.

The SDS-PAGE gels looked similar over the weeks (see appendix 4.1), apart from the new band that started appearing around 94kDa just beneath the strongest band of 104kDa thought to be the monomer. This pattern was mainly seen in the gels loaded with samples stored in 4°C. The same pattern was observed in the initial study. To further investigate this, one band of 94kDa (from week 4, tris-HCl buffer with NaCl, stored in 4°C) was cut out from the gel to be further analyzed using mass spectrometry. The band appears stronger in this well seen in figure 30b (4°C) compared to the others, which is due to it intendedly being overloaded with 2,5ug protein instead of 1ug protein, to observe the new appearing band more closely.

By comparing the ImageQuant results between the sucrose buffers and the NaCl buffers, shown in figure 31, it was seen that the monomer percentage was higher in the sucrose samples for the samples stored in -80°C. This indicates that sucrose could have a stabilizing effect on the fused protein, and it was therefore decided to move forward with one sucrose buffer to the stress study. No significant difference was seen for the samples stored in 4°C where the error bars overlap.

SE-HPLC

The same reasoning as presented in the initial study discussion remains. The peak at 27 minutes corresponds to the monomer, the peak at 24minutes representing the dimer and the last peak at 22.5 minutes to represent the trimer, see figure 32a and 32b. The intensity of the peaks between the buffers over the weeks differ a little bit, but overall the pattern is very similar in all measurements over the 5 weeks. In appendix 4.2 it can be seen that the peak at 22.5 minutes, the trimer, seems to appear and disappear between the measurements. This is thought to be due to bad separation in the column that was used and not due to any changes in the sample.

SEC-MALS

The results from the SEC-MALS measurement showed that the original protein sample consisted of four populations of different sizes, most probably corresponding to a monomer (104.8 kDa), dimer (213.3 kDa), trimer (361.1kDa) and a larger aggregate (2073.1 kDa), as seen in figure 33. From the refractive index it was found that a part of the measured molar mass (4.1kDa of the monomer, 3.4kDa of the dimer) belonged to a sugar structure and not a protein, see figure 34. This suggests that the protein complex had been glycosylated, which confirms the higher molecular weight seen in ImageQuant of the SDS-PAGE gels. This is a natural mechanism that occurs during the post translational modifications when producing the protein in baculo cells. Previous studies have shown that this type of modification can be positive both for the folding and stability of proteins. (Harrison, R. L., & Jarvis, D. L, 2006)

CSA ELISA

Overall, a lower binding towards HSPG and higher binding to decorin was seen in all samples (figures 35a, 35b and 35c compared to figures 36a, 36b and 36c), as expected. Furthermore, no major differences in binding were observed between the 4°C and -80°C samples. However, the decorin binding seems to decrease slightly over time and the HSPG binding seems to be more spread out in the measurements made in the later

weeks. These observations could be a result of stress, but it cannot be excluded that other factors such as differences in room temperature from day to day could have impacted the results.

Since no major differences were observed in this experiment, is it hard to draw any conclusions from the results regarding which buffer was most suitable for the protein.

CD3 ELISA

In the results from the CD3 ELISA experiments from week 4 (figure 37b), a large variation in binding is seen. The MES NaCl buffer and histidine sucrose buffer stored in 4°C, as well as the tris-HCl NaCl and PBS buffer stored in -80°C, all seem to have a lower binding compared to the other samples during the measurement in week 4. However, it is difficult to draw any conclusions regarding this, as it is only seen in one measurement and many external factors could have caused the lower binding. Furthermore, the -80°C tris-HCl buffer with NaCl was also an outlier during all three weeks 1, 4 and 12 measurements and was therefore excluded in the stress study, see figure 37a and 37c.

FACS

The FACS measurement showed that the rVAR2-aCD3 protein binds T-cells. In figure 38a, 38b and 38c, it is seen that all buffers follow a similar pattern during each measurement. It can also be seen that using frozen PBMCs gave rise to similar results as freshly used, even though less cells were alive in these measurements. The result also shows that protein at low concentrations has high binding, suggesting using a set-up with a maximum concentration of 200nM and a further four-fold dilution series is suitable for similar upcoming experiments.

It is seen in figures 38a, 38b and 38c that the refractive index varies from time to time. As there is very little difference between the buffers within the measurements, it is thought that this is an effect of environmental- and human factors and hence, it is not comparable between the weeks.

DLS

In figure 39, 40 and 41, it was observed that the size distribution of the particles was more spread out after heat shocking the samples. In the sample that was not heat shocked, one peak was observed, suggesting a monomodal and polydisperse solution, which was expected. After heat shock, the seen distribution indicated a more polydisperse solution. (Wyatt Technology, 2017) This suggests that the fused protein has degraded into smaller parts, seen in both the samples heat shocked at 40°C and 55°C, but also started to cluster together into larger aggregates, seen in the samples heat shocked at 55°C.

SAS JMP

Due to large sets of data obtained from all the analyzes performed, some parameters that seemed to have a greater impact on the choice of buffer were chosen to be used in the analytical computer software SAS JMP. These parameters included maximized peak% at 27 minutes from SE-HPLC, maximized band% at 104kDa from SDS-PAGE (DTT+) and minimized Kd values from CSA ELISA with decorin. The peak seen at 27 minutes in SE-HPLC and the band seen at 104kDa in SDS-PAGE both correspond to the monomer and a low Kd value corresponds to a high decorin binding.

The results from the analytical analysis show that the samples stored in -80°C seems to be more stable than the samples stored in 4°C, see figure 42. This was also supported by the results from all analytical methods. The program also suggests that pH 6 is the most stable condition for the protein of interest.

7.4 Stress study

In the following section, the results from the stress study are discussed.

NanoDSF

Similar first derivatives of the melting curves obtained from the NanoDSF results of buffers with a pH <7 having two peaks whereas buffers with a pH >7 having one peak, was seen in all three sub-studies. This indicated that stress did not have an impact on the first derivative melting curve pattern.

SDS-PAGE & MS

In the SDS-PAGE gel from the end of stress test 1 (figure 44), 7 new bands have appeared that were not seen from start (figure 43), where 6 of them appear in the wells loaded with the PBS buffer and tris-HCl sucrose buffer samples. Bands seen at lower molecular sizes could either be degradations of the protein or contaminants in the sample. Bands appearing at larger molecular weights would most probably arise from aggregates. Both degradation and aggregation can be effects from physical stress (Manning, M. C., et al. 2010).

To be able to say exactly what these new appearing bands are representing, they would need to be further investigated with complementary analytical techniques. The band seen at 104 kDa, thought to be the monomer of the protein, together with a few appearing bands at lower molecular weights (thought to be degradation products), were cut out from the gels and sent away for mass spectrometry analysis. However, as the results that came back only had detected 21.6% of the monomer band, 10.9% of the band underneath it (94kDa) and 0% of the degradation band at 70kDa, it was impossible to draw any conclusions of which parts of the protein that the degradation products belonged to. The results are found in appendices 5.1 and 9. Clearly, another technique should be considered, suggestively Western Blot, or the MS technique that was used needs further optimization in order to be used for this matter.

In the SDS-PAGE gel from the end of stress test 2 (figure 45), 6 new bands have appeared that were not seen from start (figure 43), where all appear in the wells loaded with the PBS buffer and tris-HCl sucrose buffer samples. The appearing bands are similar to the ones seen in stress test 1, indicating that the bands of lower molecular weight arise from degradation products and not contamination.

A difference between stress test 1 and stress test 2 is that the bands marked out with green arrows in stress test 1 is not seen on the gel in stress test 2. Interestingly, they seem to appear at the same molecular size as BSA, suggesting the samples could have been contaminated with BSA, although it is a bit odd that all three samples were equally contaminated. It is noteworthy that nothing shows up in the wells without DTT dye (-) either, however this could be due to the bands being quite thin in the wells with DTT (+). Further investigation is needed to draw any conclusions about this.

The other difference between the gels from stress test 1 and 2 is that the band marked with a purple arrow appears in both PBS and tris-HCl sucrose samples in stress test 2, whereas it only shows up in tris-HCl sucrose in stress test 1. First of all, it is questionable to see a larger aggregate, in the size range of a possible dimer, appearing in the well loaded with DTT dye (+). Dimers and trimers appear in the wells without DTT (-), but the bonds between the oligomers should be cleaved by the reducing agent in the wells with DTT (+). For further investigation, another reducing agent could be used in a future experiment. However, as it appears in PBS as well in stress test 2, the rotation could have had an effect on this aggregation process.

In figures 45, 46, 47 and 48 from stress tests 1 and 2, it is seen that the 104kDa band percentage (monomer) was higher from start and gradually decreased over time. In both stress tests the smallest decrease is seen in the histidine NaCl buffer. The tris-HCl and PBS samples have a similar higher decrease in stress test 2, but in stress test 1 the largest decrease is observed in the tris-HCl buffer.

These results were similar to a conclusion drawn from a study by Chavez, B. K. et al. showing that histidine NaCl buffer with arginine substantially improved the stability for long-term storage and freezing and thawing of an IgG antibody (Chavez, B. K. et al., 2015). Another study on the protein lactate dehydrogenase from Al-hussein, A., & Gieseler, H., drew the same conclusion that the histidine buffer improved the stability more than other buffers (Al-hussein, A., & Gieseler, H. 2013). However, it is important to remember that all proteins are different and thereby have their own specific formulation preferences. (Wang, W., 1999)

A change that was clear in all buffer samples from both stress test 1 and 2, was that the monomer band intensity (104kDa) seemed to decrease over time and in turn, the band of 94kDa increased, as seen in figures 44 and 47. The truncation band (94kDa) is found approximately at 10kDa lower than the monomer. This was seen in both the initial study and the tonicity study as well, but the effect was much clearer in the stress study. Hence, it is thought that as the protein is exposed to stress, a fragment around 10kDa falls off.

The SDS-PAGE gel from the end of stress test 3 showed no observed differences from the starting point, see figure 50. This indicates that the protein is not very stressed by freezing and thawing. Stress test 3 was stopped after 6 cycles of freezing and thawing as it was considered to be unlikely that the pharmaceutical would ever be exposed to this stress more times.

SE-HPLC & NanoDrop

The chromatograms obtained by SE-HPLC from stress tests 1 (figures 52a, 52b and 52c) and 2 (figures 53a, 53b and 53c) show similar results. Over time, two new peaks appear in the tris-HCl sucrose and PBS samples, one at a retention time of 29 minutes and one at 35 minutes compared to start (figures 51a, 51b and 51c). Later retention times means smaller fragments and that the peaks appear in both studies indicate that they are not contaminants, but degradation products.

In stress test 3 (figures 54a, 54b and 54c), no new peaks appeared. However, the intensity of the sample in the PBS buffer seemed to increase (figure 54b). A higher peak intensity is achieved by increased concentration which was also confirmed by the NanoDrop measurement. In NanoDrop a concentration of 0,809 mg/mL

was measured at start, whereas a concentration of 1,34 mg/mL was measured at the end of the study. An increase in protein concentration is most probably caused by evaporation leading to a decrease in the total volume. This is something that was not observed during the measurements, however the volumes that were used were around 100-200μL and to notice changes in such small volumes is very difficult by the naked eye. That the decrease was greater in the PBS buffer in comparison to the other two buffers could indicate that something in the composition of the buffer, for instance the combination of many different salts, had an increasing effect on evaporation. However, to draw any conclusions regarding this, further investigation would be needed. Also, that the concentration increase was as largest during stress test 3 could be due to freezing and thawing impacting evaporation more than standing in room temperature.

CSA ELISA

High binding towards decorin and low binding towards HSPG was seen in all the buffers from start, as expected, see figures 55a and 55b. In general, the binding does not decrease much for any of the buffers in either of the stress tests.

In stress test 1, the sample in histidine buffer with NaCl has slightly higher decorin binding, but also higher HSPG binding than the other two buffers (figure 56a and 56b). The samples with tris-HCl sucrose and PBS have very similar binding. The plot over the HSPG binding looks very similar between stress tests 1 and 2. In the decorin binding of stress test 2 (figure 57a), the different buffers differ slightly in binding, where histidine has the highest binding, followed by PBS buffer and the lowest binding is seen in the tris-HCl buffer. The results from stress test 3 (figure 58a and b) look very similar to the binding seen at start, indicating that the binding was not impacted by freezing and thawing.

In the SDS-PAGE gels from the end of stress studies 1 and 2 it was seen that a fragment around 10kDa falls off after being exposed to stress. However, as the binding towards decorin and HSPG does not seem to be greatly impacted, this fragment is probably not located near the CSA binding site of the protein and might therefore not have a negative effect on the pharmaceutical effect.

NGC

Since only very low concentrations of the fractionated monomers and dimers could be obtained from the NGC, the analytical methods performed on the fractions (SDS-PAGE, SE-HPLC and ELISA) could not give any valuable information. The results are found in appendix 10. However, it was seen that NGC could be used to separate monomers from dimers and further analysis on their respective behavior and binding would be interesting to investigate in a future study. In order to do this, a higher concentration of the protein would be needed as the samples are diluted during the NGC measurement.

8. Conclusions

Conclusions that have been drawn upon the results and discussions are presented below.

8.1 *In silico* modelling

The consultancy firm CMC Assist developed an *in silico* model of the 3D structure of the rVAR2-aCD3 protein. To evaluate the accuracy of this model, complementary analytical techniques to determine the protein structure are needed.

8.2 Initial study

It was concluded to not proceed with the citrate buffer (pH 3.3) nor the acetate buffer (pH 4.5) as no benefits with using a lower pH formulation could be found. It was further concluded that in the upcoming experiments the samples would not be repeatedly frozen and thawed for new measurements, but instead aliquots would be prepared. In addition, it was decided to only analyze one parameter at a time. Also, -80°C seemed to be the better choice of temperature for storage.

8.3 Tonicity study

In all analytical methods used, it was seen that the samples stored in -80°C were more stable than the samples stored in 4°C. Furthermore, it was decided to continue with 3 buffers from the tonicity study to the upcoming stress study. tris-HCl with sucrose was chosen as candidate due to keeping a high monomer percentage over the weeks and showing high CD3 binding during all measurements. The optimal pH suggested by SAS JMP was pH 6, and hence the histidine buffer with NaCl was chosen as second candidate. The last candidate was the buffer the protein originally had been stored in, PBS, due to being commonly used in the industry and showing good results in the analytical assays.

8.4 Stress study

The protein showed to be stable in all three formulations towards freeze and thawing, at least up to 6 times. Furthermore, it was found that the histidine buffer with NaCl was the most stress resistant towards storage in room temperature and rotation. In the PBS and tris-HCl sucrose samples, more degradation products and aggregates appeared upon induced stress, which was not observed in the histidine NaCl sample. Furthermore, the histidine buffer with NaCl kept the highest monomer percentage over time.

8.5 Final conclusions & future perspectives

The aim of this project was to select the best candidate for a frozen-liquid rVAR2-aCD3 formulation to support clinical phase I studies. After testing various buffers using a range of different analytical techniques, the histidine NaCl buffer showed most promising results, stored in -80°C.

The next step would be to optimize the formulation further to prevent chemical degradation. The amino acid map from the *in silico* analysis of the scFv of aCD3, showed potential risks of deamidation, oxidation and light induced oxidation. A lower pH prevents deamidation, supporting the choice of histidine buffer (Wang,

W.,1999). Further formulation development could include adding antioxidants and the pharmaceutical could be considered to be kept in non-transparent containers. A similar amino acid map should also be created for the VAR2-part of the protein once the exact binding regions have been discovered and more formulation improvements could be suggested based upon those results.

9. Acknowledgements

We would like to give a special thank you to the companies VAR2 Pharmaceuticals and CMC Assist for giving us the opportunity to carry through with this project in the middle of a global pandemic. Thank you Ali Salanti for your encouragement and for doing your most to let us proceed with our work during the arising restrictions. Thank you Swati Choudhary for having patience, for always supporting us and teaching us to think and work as biotechnical engineers. We would also like to thank the rest of the employees at the laboratory department CMP for their kindness and help in every tricky situation. Furthermore, we wish to thank Jens Bukrinski and Mette Hamborg from CMC Assist for advice, planning and constructive discussions throughout the whole process. We would also like to thank our supervisor from LTH, Jenny Schelin, and examiner, Marie Wahlgren, for guidance and answering questions.

Finally, we wish to thank our families and friends for their support during our studies.

10. References

10.1 Articles

1. Al-hussein, A., & Gieseler, H. (2013). Investigation of histidine stabilizing effects on LDH during freeze-drying. Journal of Pharmaceutical Sciences, 102(3), 813–826. https://doi.org/10.1002/jps.23427
2. Amin, S., Barnett, G. V., Pathak, J. A., Roberts, C. J., & Sarangapani, P. S. (2014, October 1). Protein aggregation, particle formation, characterization & rheology. Current Opinion in Colloid and Interface Science. Elsevier Ltd. https://doi.org/10.1016/j.cocis.2014.10.002
3. Baek, Y., Singh, N., Arunkumar, A., & Zydney, A. L. (2017). Effects of Histidine and Sucrose on the Biophysical Properties of a Monoclonal Antibody. Pharmaceutical Research, 34(3), 629–639. https://doi.org/10.1007/s11095-016-2092-0
4. Chavez, B. K., Agarabi, C. D., Read, E. K., Boyne, M. T., Khan, M. A., & Brorson, K. A. (2016). Improved stability of a model IgG3 by DoE-based evaluation of buffer formulations. BioMed Research International, 2016. https://doi.org/10.1155/2016/2074149
5. Chen, B., Bautista, R., Yu, K., Zapata, G. A., Mulkerrin, M. G., & Chamow, S. M. (2003). Influence of Histidine on the Stability and Physical Properties of a Fully Human Antibody in Aqueous and Solid Forms. *Pharmaceutical Research*, *20*(12), 1952–1960. https://doi.org/10.1023/B:PHAM.0000008042.15988.c0
6. Christianson, H. C., & Belting, M. (2014). Heparan sulfate proteoglycan as a cell-surface endocytosis receptor. *Matrix Biology,* 35, 51–55. https://doi.org/10.1016/j.matbio.2013.10.004
7. Clausen, T. M., Christoffersen, S., Dahlbäck, M., Langkilde, A. E., Jensen, K. E., Resende, M., ... Salanti, A. (2012). Structural and functional insight into how the Plasmodium falciparum VAR2CSA protein mediates binding to chondroitin sulfate A in placental malaria. Journal of Biological Chemistry, 287(28), 23332–23345. https://doi.org/10.1074/jbc.M112.348839
8. Duerr, C., & Friess, W. (2019, June 1). Antibody-drug conjugates- stability and formulation. European Journal of Pharmaceutics and Biopharmaceutics. Elsevier B.V. https://doi.org/10.1016/j.ejpb.2019.03.021
9. Elias, C. B., & Joshi, J. B. (1998). Role of hydrodynamic shear on activity and structure of proteins. *Advances in Biochemical Engineering/Biotechnology*. https://doi.org/10.1007/bfb0102296
10. Harrison, R. L., & Jarvis, D. L. (2006). Protein N-Glycosylation in the Baculovirus-Insect Cell Expression System and Engineering of Insect Cells to Produce "Mammalianized" Recombinant Glycoproteins. *Advances in Virus Research*. https://doi.org/10.1016/S0065-3527(06)68005-6
11. Hauptmann, A., Podgoršek, K., Kuzman, D., Srčič, S., Hoelzl, G., & Loerting, T. (2018). Impact of Buffer, Protein Concentration and Sucrose Addition on the Aggregation and Particle Formation during Freezing and Thawing. Pharmaceutical Research, 35(5). https://doi.org/10.1007/s11095-018-2378-5
12. Hayakawa, E. H., & Matsuoka, H. (2016). Detailed methodology for high resolution scanning electron microscopy (SEM) of murine malaria parasitized-erythrocytes. Parasitology International, 65(5), 539–544. https://doi.org/10.1016/j.parint.2016.03.006

13. Higgins, M. K. (2008). The structure of a chondroitin sulfate-binding domain important in placental malaria. *Journal of Biological Chemistry*, *283*(32), 21842–21846. https://doi.org/10.1074/jbc.C800086200
14. Huehls, A. M., Coupet, T. A., & Sentman, C. L. (2015, March 19). Bispecific T-cell engagers for cancer immunotherapy. Immunology and Cell Biology. Nature Publishing Group. https://doi.org/10.1038/icb.2014.93
15. Kipriyanov, S. M., Moldenhauer, G., Martin, A. C. R., Kupriyanova, O. A., & Little, M. (1997). Two amino acid mutations in an anti-human CD3 single chain Fv antibody fragment that affect the yield on bacterial secretion but not the affinity. Protein Engineering, 10(4), 445–453. https://doi.org/10.1093/protein/10.4.445
16. Kwan, T. O. C., Reis, R., Siligardi, G., Hussain, R., Cheruvara, H., & Moraes, I. (2019, May 27). Selection of Biophysical Methods for Characterisation of Membrane Proteins. International Journal of Molecular Sciences. NLM (Medline). https://doi.org/10.3390/ijms20102605
17. Le Basle, Y., Chennell, P., Tokhadze, N., Astier, A., & Sautou, V. (2020, January 1). Physicochemical Stability of Monoclonal Antibodies: A Review. *Journal of Pharmaceutical Sciences*. Elsevier B.V., https://doi.org/10.1016/j.xphs.2019.08.009
18. Lee, J. C., & Timasheff, S. N. (1981). The stabilization of proteins by sucrose. Journal of Biological Chemistry, 256(14), 7193–7201. https://doi.org/10.1016/S0021-9258(19)68947-7
19. Mao, Y. J., Sheng, X. R., & Pan, X. M. (2007). The effects of NaCl concentration and pH on the stability of hyperthermophilic protein Ssh10b. BMC Biochemistry, 8. https://doi.org/10.1186/1471-2091-8-28
20. Manning, M. C., Chou, D. K., Murphy, B. M., Payne, R. W., & Katayama, D. S. (2010, April). Stability of protein pharmaceuticals: An update. *Pharmaceutical Research*. https://doi.org/10.1007/s11095-009-0045-6
21. Mauri, C., & Bosma, A. (2012). Immune regulatory function of B cells. *Annual Review of Immunology*. https://doi.org/10.1146/annurev-immunol-020711-074934
22. Moman, R. N., & Varacallo, M. (2019). Physiology, Albumin. StatPearls. Retrieved from http://www.ncbi.nlm.nih.gov/pubmed/29083605
23. Nordmaj, M. A., Roberts, M. E., Sachse, E. S., Dagil, R., Andersen, A. P., Skeltved, N., Grunddal, K. V., Erdoğan, S. M., Choudhary, S., Gustavsson, T., Ørum-Madsen, M. S., Moskalev, I., Tian, W., Yang, Z., Clausen, T. M., Theander, T. G., Daugaard, M., Nielsen, M. A., & Salanti, A. (2021). Development of a bispecific immune engager using a recombinant malaria protein. Cell death & disease, 12(4), 353. https://doi.org/10.1038/s41419-021-03611-0
24. Pramanik, K., Ghosh, P. K., Ray, S., Sarkar, A., Mitra, S., & Maiti, T. K. (2017). An in silico structural, functional and phylogenetic analysis with three dimensional protein modeling of alkaline phosphatase enzyme of Pseudomonas aeruginosa. *Journal of Genetic Engineering and Biotechnology*, *15*(2), 527–537. https://doi.org/10.1016/j.jgeb.2017.05.003
25. Reszegi, A., Horváth, Z., Fehér, H., Wichmann, B., Tátrai, P., Kovalszky, I., & Baghy, K. (2020). Protective Role of Decorin in Primary Hepatocellular Carcinoma. Frontiers in Oncology, 10. https://doi.org/10.3389/fonc.2020.00645

26. Roberts, C. J., Das, T. K., & Sahin, E. (2011). Predicting solution aggregation rates for therapeutic proteins: Approaches and challenges. *International Journal of Pharmaceutics*, *418*(2), 318–333. https://doi.org/10.1016/j.ijpharm.2011.03.064
27. Salanti, A., Clausen, T. M., Agerbæk, M. O., Al Nakouzi, N., Dahlbäck, M., Oo, H. Z., ... Daugaard, M. (2015). Targeting Human Cancer by a Glycosaminoglycan Binding Malaria Protein. Cancer Cell, 28(4), 500–514. https://doi.org/10.1016/j.ccell.2015.09.003
28. Stetefeld, J., McKenna, S. A., & Patel, T. R. (2016,). Dynamic light scattering: a practical guide and applications in biomedical sciences. *Biophysical Reviews*. Springer Verlag. https://doi.org/10.1007/s12551-016-0218-6
29. Stone, J. (2017) Chapter 3 - Sample preparation techniques for mass spectrometry in the clinical laboratory, Editor(s): Hari Nair, William Clarke, Mass Spectrometry for the Clinical Laboratory, Academic Press, Pages 37-62 https://doi.org/10.1016/B978-0-12-800871-3.00003-1
30. Temel, D. B., Landsman, P., & Brader, M. L. (2016). Orthogonal Methods for Characterizing the Unfolding of Therapeutic Monoclonal Antibodies: Differential Scanning Calorimetry, Isothermal Chemical Denaturation, and Intrinsic Fluorescence with Concomitant Static Light Scattering. In *Methods in Enzymology* (Vol. 567, pp. 359–389). Academic Press Inc. https://doi.org/10.1016/bs.mie.2015.08.029
31. Thakkar, S. V., Joshi, S. B., Jones, M. E., Sathish, H. A., Bishop, S. M., Volkin, D. B., & Middaugh, C. R. (2012). Excipients differentially influence the conformational stability and pretransition dynamics of two IgG1 monoclonal antibodies. *Journal of Pharmaceutical Sciences*, *101*(9), 3062–3077. https://doi.org/10.1002/jps.23187
32. Thorat, A. A., & Suryanarayanan, R. (2019). Characterization of Phosphate Buffered Saline (PBS) in Frozen State and after Freeze-Drying. *Pharmaceutical Research*, *36*(7). https://doi.org/10.1007/s11095-019-2619-2
33. Van den Berg, L., & Rose, D. (1959). Effect of freezing on the pH and composition of sodium and potassium phosphate solutions: the reciprocal system KH2PO4Na2HPO4H2O. *Archives of Biochemistry and Biophysics*, *81*(2), 319–329. https://doi.org/10.1016/0003-9861(59)90209-7
34. Wang, W. (1999, August 20). Instability, stabilization, and formulation of liquid protein pharmaceuticals. International Journal of Pharmaceutics. https://doi.org/10.1016/S0378-5173(99)00152-0
35. Wöll, A. K., & Hubbuch, J. (2020). Investigation of the reversibility of freeze/thaw stress-induced protein instability using heat cycling as a function of different cryoprotectants. *Bioprocess and Biosystems Engineering*, *43*(7), 1309–1327. https://doi.org/10.1007/s00449-020-02327-3
36. Yancey, P. H. (2005, August). Organic osmolytes as compatible, metabolic and counteracting cytoprotectants in high osmolarity and other stresses. Journal of Experimental Biology. https://doi.org/10.1242/jeb.01730
37. Yang, M. (2015). Stress and protein instability during formulation and fill/finish processes. BioPharm International, 28(6), 46–47
38. Ziessman, H. A., O'Malley, J. P., & Thrall, J. H. (2006). Infection and Inflammation. In *Nuclear Medicine* (pp. 384–418). Elsevier. Accessed: 2021-04-14, Retrieved from: https://doi.org/10.1016/b978-0-323-02946-9.50017-9

10.2 Websites

1. GenBank (2009) *Synthetic construct VAR2CSA gene, exon 1 and partial cds,* Accessed: 2021-02-22, Retrieved from: https://www.ncbi.nlm.nih.gov/nuccore/GU249598
2. National Cancer Institute (2019) *Immunotherapy to Treat Cancer,* Accessed: 2020-12-22, Retrieved from: https://www.cancer.gov/about-cancer/treatment/types/immunotherapy
3. The Nobel Prize, (2018), *Press release: The Nobel Prize in Physiology or Medicine 2018*, Accessed: 2021-01-21, Retrieved from: https://www.nobelprize.org/prizes/medicine/2018/press-release/
4. University of Copenhagen (2020), *From a malaria Ph.D. to a possible cure for cancer*, Faculty of Health and Medical Sciences, Accessed: 2020-11-05, Retrieved from: https://healthsciences.ku.dk/about/impact/basic-research/ali-salanti/
5. VAR2 pharmaceuticals (2020), *Research & development*, Accessed: 2020-11-18, Retrieved from: https://var2pharma.com/reasearch-development/
6. World health organization, (2020), *The top 10 causes of death*, Accessed: 2021-01-21, Retrieved from: https://www.who.int/news-room/fact-sheets/detail/the-top-10-causes-of-death

10.2.1 Method & Material references

7. AATbioquest (2020), *Citrate Buffer (pH 3.0 to 6.2) Preparation and Recipe*, Accessed: 2020-12-08, Retrieved from: https://www.aatbio.com/resources/buffer-preparations-and-recipes/citrate-buffer-ph-3-to-6-2
8. AATbioquest (2020), *Acetate Buffer (pH 3.6 to 5.6) Preparation and Recipe*, Accessed: 2020-12-08, Retrieved from: https://www.aatbio.com/resources/buffer-preparations-and-recipes/acetate-buffer-ph-3-6-to-5-6
9. AATbioquest (2020), *MES (0,5M, pH 6) Preparation and Recipe*, Accessed: 2020-12-08, Retrieved from: https://www.aatbio.com/resources/buffer-preparations-and-recipes/mes-ph-6
10. Biocompare (2003), *NanoDrop Spectrophotometer from NanoDrop Technologies*, Accessed: 2020-12-14, Retrieved from: https://www.biocompare.com/Product-Reviews/41288-NanoDrop-Spectrophotometer-from-NanoDrop-Technologies/
11. Bio-rad (2020), *Desalting Column*, Accessed: 2020-12-10, Retrieved from: https://www.bio-rad.com/featured/en/desalting-column.html
12. Bio-rad (2021), *NGC Chromatography Platform*, Accessed: 2021-03-25, Retrieved from: https://info.bio-rad.com/NGCPHA-lp1.html?ovl5&WT.mc_id=180927025184#N3
13. BOSTER antibody and ELISA experts (2020), *ELISA principle*, Accessed: 2020-12-10, Retrieved from: https://www.bosterbio.com/protocol-and-troubleshooting/elisa-principle
14. Coriolis Pharma (2020), *Nano differential scanning fluorimetry (nanoDSF / nDSF)*, Accessed: 2020-12-14, Retrieved from: https://www.coriolis-pharma.com/analytical-services/higher-order-structure/nano-differential-scanning-fluorimetry-nanodsf-ndsf
15. JMP Statistical discovery from SAS (2013), *Basic JMP vs SAS overview?,* Accessed: 2020-12-18, Retrieved from: https://community.jmp.com/t5/Discussions/Basic-JMP-vs-SAS-overview/td-p/7503#

16. Merck (2021), *1X PBS (Phosphate-Buffered Saline) Recipe Calculator*, Accessed: 2021-03-22, Retrieved from: https://www.sigmaaldrich.com/technical-documents/protocols/biology/western-blotting/buffers-recipes/1x-phosphate-buffered-saline.html
17. Merck (2021), *Biological Buffer Selection Guide*, Accessed: 2021-02-18, Retrieved from:https://www.sigmaaldrich.com/life-science/core-bioreagents/biological-buffers.html
18. Merck (2021) *Bovine Serum Albumins*, Accessed: 2021-04-06, Retrieved from: https://www.sigmaaldrich.com/life-science/biochemicals/biochemical-products.html?TablePage=103994915
19. MSU Chemistry (2013) *Biological Buffer Selection Guide*, Accessed: 2021-02-18, Retrieved from: https://www2.chemistry.msu.edu/faculty/reusch/VirtTxtJml/Spectrpy/MassSpec/masspec1.htm?ref=sexshop06.net
20. Paar, A. (2021) *The principles of dynamic light scattering,* Accessed: 2021-02-23, Retrieved from: *https://wiki.anton-paar.com/en/the-principles-of-dynamic-light-scattering/*
21. Protein data bank (2021), *Methods for Determining Atomic Structures,* Accessed: 2021-04-01, Retrieved from: https://pdb101.rcsb.org/learn/guide-to-understanding-pdb-data/methods-for-determining-structure
22. Protocols Online (2016), *Phosphate buffered saline*, Accessed: 2020-12-08, Retrieved from: https://www.protocolsonline.com/recipes/phosphate-buffered-saline-pbs/
23. PyMOL (2021), *PyMOL by Schrrödinger*, Accessed: 2021-02-18, Retrieved from: https://pymol.org/2/
24. Sciencing (2018), W*hat Is the Function of a Tris Buffer in DNA Extraction?,* Accessed: 2020-12-09, Retrieved from: https://sciencing.com/function-tris-buffer-dna-extraction-6370973.html
25.
26. Tebu Bio (2017), *How to choose the perfect buffer to get a pure, stabilised, functional protein*, Accessed: 2020-12-09, Retrieved from: https://www.tebu-bio.com/blog/2017/01/30/how-to-choose-easily-the-perfect-buffer-to-purify-and-obtain-a-pure-stabilized-and-functional-protein/
27. Thermofisher (2020), *DTT (dithiothreitol)*, Accessed: 2020-12-21, Retrieved from: https://www.thermofisher.com/order/catalog/product/R0861#/R0861
28. Wyatt Technology, (2021), *SEC-MALS*, Accessed: 2021-02-18, Retrieved from: https://www.wyatt.com/solutions/techniques/sec-mals-molar-mass-size-multi-angle-light-scattering.html
29. 2 bind molecular interactions (2020), *The gold standard for challenging protein stability*, Accessed: 2020-12-18, Retrieved from: https://2bind.com/nanodsf/

10.2.2 Figure references

30. Creative proteomics (2021), *Protein Structure Analysis Service,* Accessed: 2021-03-22, Retrieved from: https://www.creative-proteomics.com/services/protein-structure-analysis-service.htm
31. Encyclopædia Britannica, Inc. (2021) *Antibody,* Accessed: 2021-03-18, Retrieved from: https://www.britannica.com/science/antibody
32. Experiment (2016) *How does SDS-PAGE work?*, Accessed: 2020-12-10, Retrieved from: https://experiment.com/u/2WbQ0Q

33. Immunology (2016), *Immunoglobulins and T cell receptor Differences*, Accessed: 2020-12-22, Retrieved from: https://andrewimmunology.wordpress.com/2016/01/15/immunoglobulins-and-t-cell-receptor-differences/
34. MBL Life Science (2017) *The principle and method of ELISA*, Accessed: 2020-12-10, Retrieved from: https://ruo.mbl.co.jp/bio/e/support/method/elisa.html
35. Lösungsfabrik (2017), *The HPLC system: simply explained*, Accessed: 2020-12-10, Retrieved from: http://www.mpl.loesungsfabrik.de/en/english-blog/high-performance-liquid-chromatography/hplc-system-simply-explained
36. Oncobites (2019) *Sneaking into the non-conventional niches: Using gamma delta T cells to fight cancer*, Accessed: 2021-03-17, Retrieved from: https://oncobites.blog/2019/02/19/sneaking-into-the-non-conventional-niches-using-gamma-delta-t-cells-to-fight-cancer/
37. SinoBiological (2020), *Fluorescence-activated Cell Sorting (FACS)*, Accessed: 2020-12-08, Retrieved from:https://www.sinobiological.com/category/fcm-facs-facs
38. Wyatt Technology (2017), *TN2005: Cumulants versus Regularization Analysis,* Accessed: 2021-02-24, Retrieved from: https://www.wyatt.com/blogs/discover-tricks-and-tips-with-our-technical-notes.html

10.4 Online books

1. Bruce M. Koeppen MD, PhD, Bruce A. Stanton PhD (2013) *Physiology of Body Fluids*, in Renal Physiology (Fifth Edition), Pages: 1-14, Accessed: 2021-01-05, Retrieved from: https://www.sciencedirect.com/topics/immunology-and-microbiology/osmolarity-and-osmolality

10.5 Videos

1. Hack Dentistry (2017), *How do T-cells recognize antigens?*, Accessed: 2020-12-22, Retrieved from: https://www.youtube.com/watch?v=l-RCISjrFOo